ISSN 0736-5306

SCIENCE OF TSUNAMI HAZARDS

The International Journal of The Tsunami Society

Volume 10 Number 1 1992

SPECIAL ISSUE

EUROPEAN GEOPHYSICAL SOCIETY 1992 TSUNAMI MEETING

Alastair Dawson, Editor

OBJECTIVE: **The Tsunami Society** publishes this journal to increase and disseminate knowledge about tsunamis and their hazards.

DISCLAIMER: Although these articles have been technically reviewed by peers, **The Tsunami Society** is not responsible for the veractiy of any statement, opinion or consequences.

EDITORIAL STAFF

Submit manuscripts of articles, notes or letters to the Technical Editor. If an article is accepted for publication the author(s) must submit a camera ready manuscript in the journal format. A voluntary $50.00 page charge will include 50 reprints.

SUBSCRIPTION INFORMATION: Price per copy $20.00 USA

ISSN 0736-5306

Published by The Tsunami Society in Honolulu, Hawaii, USA

ASSESSING THE TSUNAMI RISK USING INSTRUMENTAL AND HISTORICAL RECORDS

José Z.Simões[1][2], Alexandra Afilhado[1][3], L.Mendes Victor[1][2]

[1] Centro de Geofísica da Universidade de Lisboa
[2] Departamento de Física da Faculdade de Ciências de Lisboa
R. Escola Politécnica 58
P-1294 Lisboa Codex PORTUGAL
[3] Instituto Superior de Engenharia de Lisboa
R. Concelheiro Imídio Navarro
P-1900-Lisboa PORTUGAL

Abstract

Portugal mainland and adjacent ocean domain, have a well documented, 2000 years old, history of strong earthquakes and destructive tsunamis originated in the "Gorringe Bank", probably the most important tsunamigenic area in Europe.

Assessing the risk of a tsunami in that area is mainly to answer to two questions: Which is the lowest seismic magnitude, able to generate a destructive tsunami? Which is the probability of occurrence of an earthquake with magnitude equal to or greater than that value? Since only a small fraction of events generating tsunamis occurred this century, we had to use historical data to try to answer those two questions.

Reports and chronicles of the damages and casualties in different locations, had allowed the estimation of epicentral position and magnitude of historical seisms, and the magnitude of the tsunami that they have generated, allowing an estimate of the lowest magnitude able to generate destructive tsunamis.

Evaluating the probability of an occurrence of such earthquakes is a complex task. Mixing historical and instrumental records, we are probably over representing earthquakes of great magnitudes.

In order to work out the problem, a "Historical Sensibility Function" has been created. That function is supposed to represent the first time that each magnitude could have been recorded. The number of occurrences of earthquakes in a given interval of magnitudes is, for subsequent computations, weighted, with the use of the "Historical Sensibility Function".

The weighted data shows a good agreement with the Gutenberg-Richter relation, for magnitudes greater than 3.0. The parameters of that relation, computed with the weighted data, have been used to evaluate the seismic and tsunami hazard.

In the southern Atlantic coast of Iberia, several destructive tsunamis occurred in the past. The Lisbon 1755 earthquake has generated, probably the largest one.

In order to assess the tsunami risk we had to use historical information, because no local or regional earthquake generating damaging tsunami has been recorded by regional networks, although the portuguese network have been installed in the beginning of the century (Silveira et al., 1991). So, we have been forced and able to collect and gather all the available information, in an alphanumerical and graphical data base (Simões et al., 1991). In many cases, using the reports of the damaging effects of the earthquakes, its magnitude and epicentral location has been estimated. Tsunami effects, when documented in historical reports, were also included in the data base. In figure 1, we can see a graphical display, of all events with available epicentral location.

Being aware of the incompleteness of the data base, we can however conclude that the seismic events generating destructive tsunamis are located inside a box, centered in a geographical point: longitude 10° W, latitude 35.5 ° N (see figure 1).

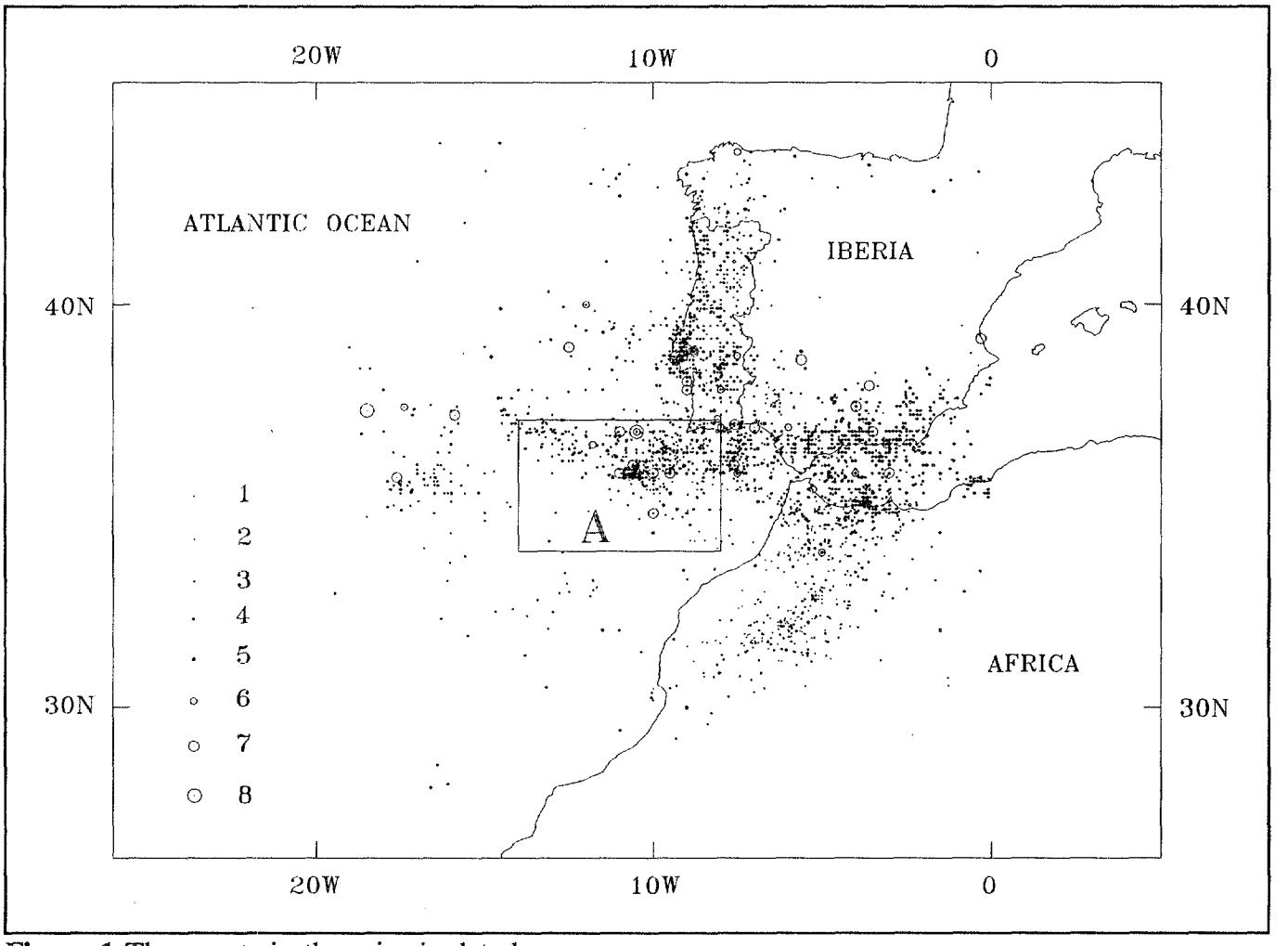

Figure 1 The events in the seismic data base.

From that data, can also be considered that an event originated in that area, with a 7.5 magnitude will generate a small tsunami, but an 8.0 event will generate a tsunami, able to cause destruction in the sea and costal areas. An 8.5 magnitude earthquake will generate a very destructive tsunami, affecting large part of Lisbon, as happened in 1755 (the estimated magnitude of that earthquake is 8.5). A 9.0 event will certainly give origin to very high devastation, but the only event reported, in our data base, candidate to that magnitude, in the 1st century B.C., is not very well documented.

Given the seismic magnitudes needed to generated destructive tsunamis, we have used the data base to estimate the probability of occurrence of such events, in a given time interval.

Trying to answer to that fundamental question, has not shown to be an easy task.

Since we have just a few instrumental records with magnitude greater than 7.5, we have to use historical events, to assess the risk.

However historical records are, most likely, biased, with an overrepresentation of events with larger magnitudes. Small earthquakes, even if felt, have been, most likely, unrecorded.

To compensate that bias we have postulate the existence of a function we called "Historical Sensibility Function" (HSF), for each relatively homogeneous region in the area of study. That function is defined, for each magnitude and for each region, as the first time an event, with magnitude equal to the given magnitude and originated in the given region, could have been recorded.

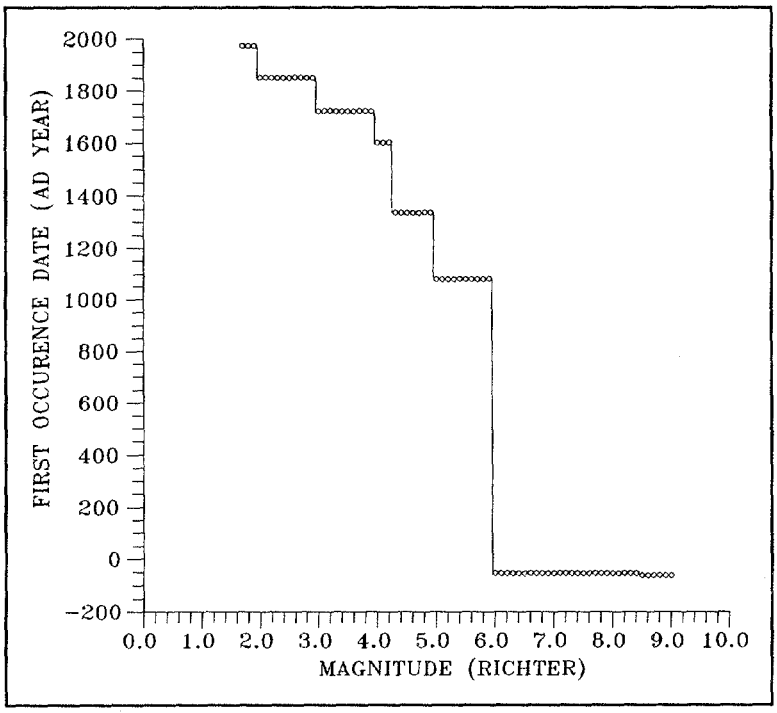

Figure 2 An estimate of the historical sensibility function (HSF).

Although, we are mainly interested in events with magnitude greater than 7.5, the HSF is defined for all magnitudes.

We have expressed the HSF in "A.D. years". For example HSF(5) = 1300 in an area, means that records made before 1300 A.D. take only in account the earthquakes in the area if their magnitude is greater than 5. We can expect that HSF(m) $\geq$ HSF(m') if m $<$ m', i.e., HSF never increases.

For each area we have roughly estimate HSF(m), for each m, as the date of the earliest event, in our data base, with epicenter in the area and magnitude equal to or less than m. Figure 2 shows an estimate of the HSF.

We have used the HSF for weighting the number of earthquakes. For each magnitude class and each area considered, we had to multiply the number of events, in that class, by the time range of the data base and divide by the difference between the date of the most recent event, in the data base, and the HSF of the central magnitude of the class.

The weighted number of events, for each class, is an estimate of the number of earthquakes that would have been recorded, if a seismic network, as the present one, would have existed during the time extent of the data, assuming that the number of events, in a certain period, follows a Poisson distribution.

In figure 3 we represented the weighted frequencies for all the events in the data base, using a semi-logarithm graph. The data fits very well a straight line. That is in good agreement with the Gutenberg-Richter law (G.-R.), and is a good argument in favor of the described methodology.

Should also be noted that the straight lines computed using the least square criteria and the maximum-likelihood criteria are virtually identical.

We have used only magnitudes equal or greater than 3, in the evaluation of the G.-R. parameters, because the data base suggest that the actual network does not always records well those magnitudes. Although, data related to all magnitudes with recorded events is shown.

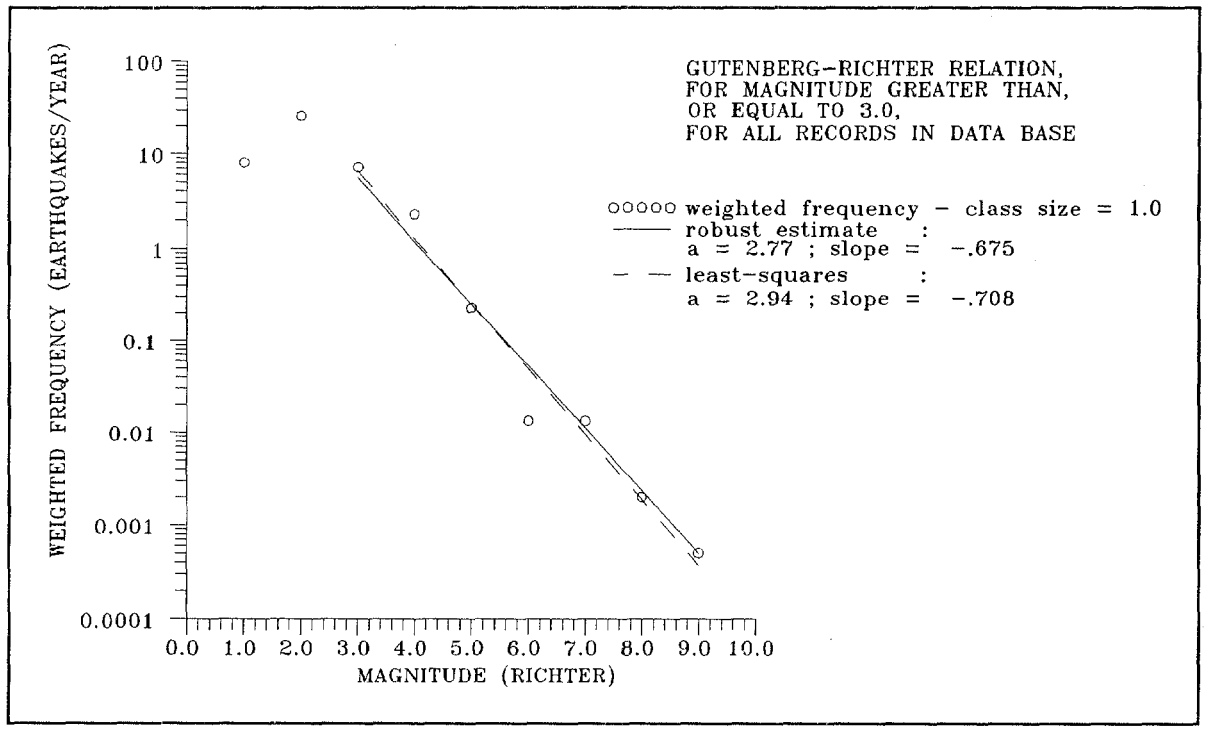

Figure 3 Gutenberg-Richter relation, for all records in figure 1.

In figure 4 we can see the G.-R. relation applied only to earthquakes with epicenter in the area "A" as seen in figure 1. That area includes the tsunamigenic spot. Again the data fits well the theoretical relation G.-R.

In figure 5, the relations to both studied areas are shown. It is clear from that figure that the two straight lines are almost parallel, slightly converging for high magnitudes.

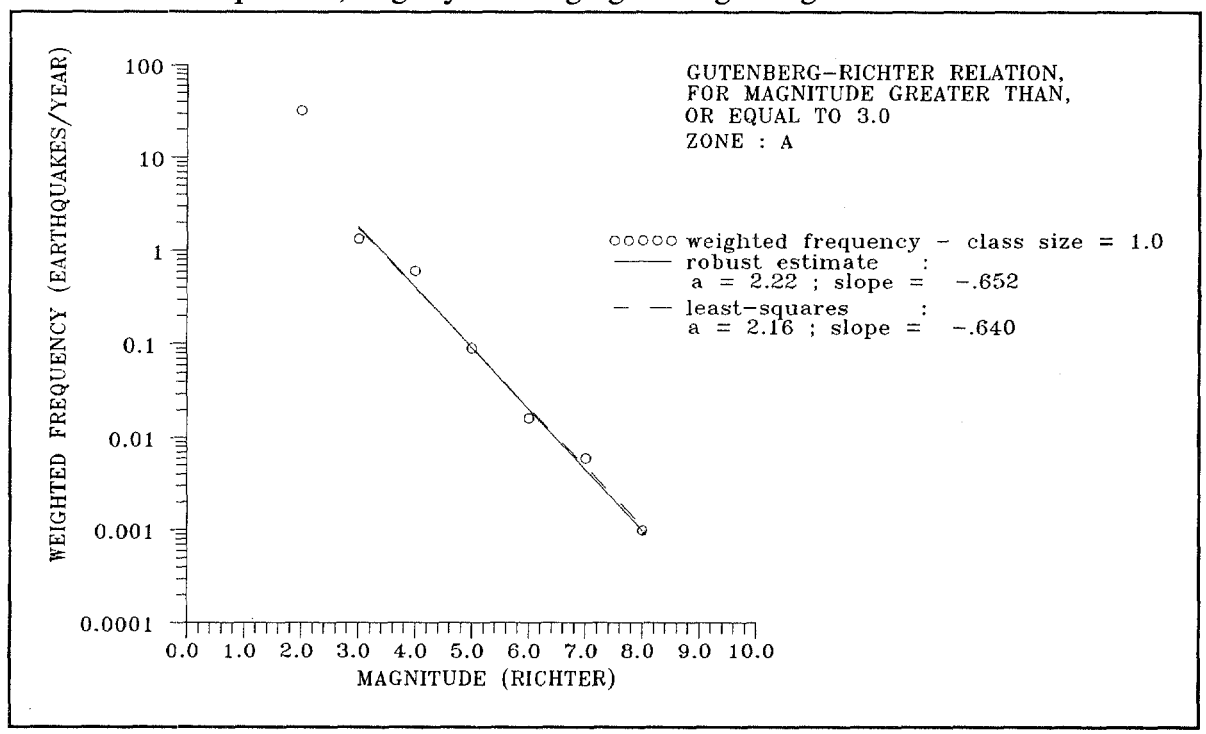

Figure 4 Gutenberg-Richter relation, for records in area "A".

However the data base contains a lot of events without known location; some of these events were originated, most likely, in the area "A". If, in figure 5, we had included those events for area "A", the two lines would have been closer.

As a result we have decided to use all the events in assessing the seismic and tsunami risk. Doing that we are probably overestimating the risk.

Some of the earthquakes that have generated destructive tsunamis have estimated magnitudes with resolution around 0.5, in the records of the data base. So, we have considered a possible error of 0.25 in the magnitude of earthquakes triggering a certain type of tsunami.

For example, our data base shows that a destructive tsunami is generated by an earthquake with magnitude 8.0 or greater, as stated before. We computed the probability of an earthquake with magnitude greater than 7.75 to assess the risk of such event.

According to that we have used the G.-R. parameter for all the records in the data base and reach the following conclusions about the tsunami risk:

Tsunami
magnitude 7.5
every 200 years

Destructive Tsunami
magnitude 8.0
every 450 years

Very destructive tsunami
magnitude 8.5
every 1000 years

Exceptional tsunami
magnitude 9.0 (?)
every 2500 years

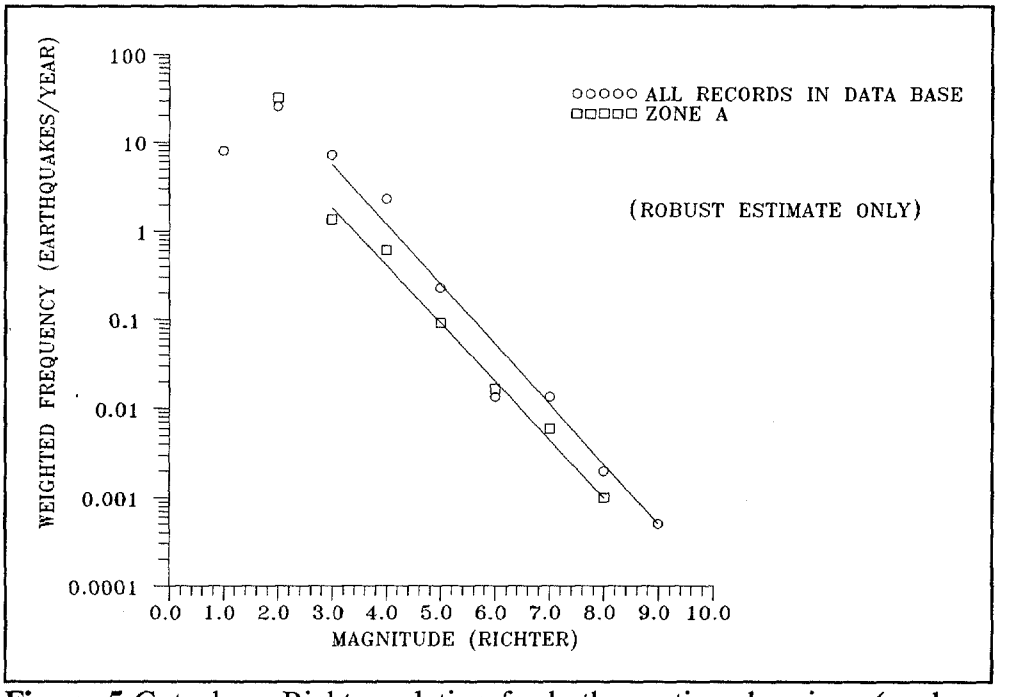

Figure 5 Gutenberg-Richter relation for both mentioned regions (we have not normalized by the area).

The quality of the achieved results, will be increased with the enlargement and improvement of our data base.

References:

Silveira, Graça M., José Z. Simões, L. Mendes Victor, "Portuguese Seismic Network", Proceedings of the I Workshop on: MEDNET, The Broad-Band Seismic Network for the Mediterranean. CCSEM, Erice, Sicily; 1991.

Simões, José Z., Graça M.Silveira, L. Mendes Victor, I. Martins, "A Data Base for Historical and Instrumental Earthquakes in Portugal", IUGG General Assembly, Vienna 1991.

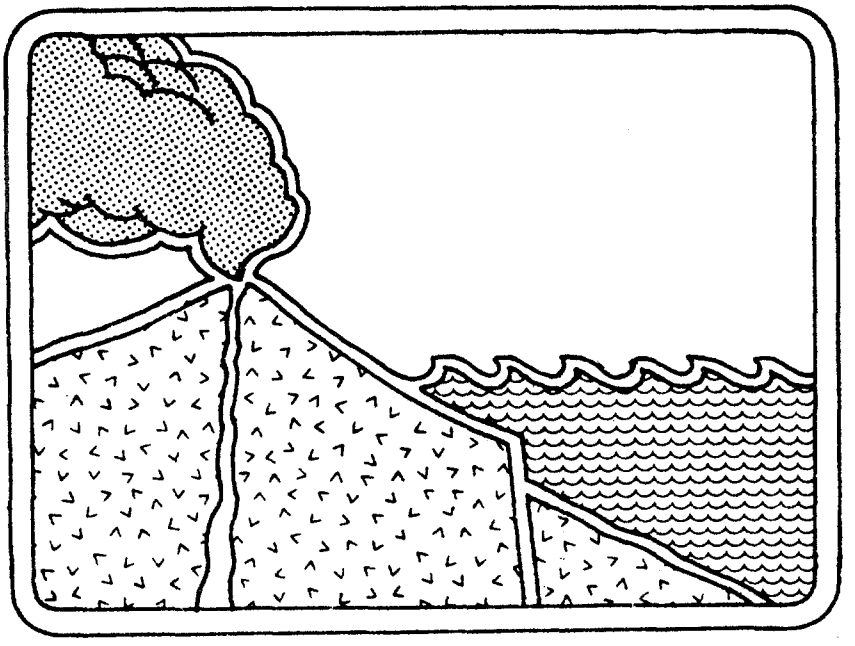

MAXIMUM ENTROPY ANALYSIS OF PORTUGUESE TSUNAMI DATA THE TSUNAMIS OF 28.02.1969 AND 26.05.1975

MARIA ANA BAPTISTA*, PEDRO MIRANDA* **, LUIS MENDES VICTOR* **

*CENTRO DE GEOFISICA DA UNIVERSIDADE DE LISBOA
** DEPT. DE FISICA DA UNIVERSIDADE DE LISBOA
R. DA ESCOLA POLITÉCNICA 58, 1200 LISBOA PORTUGAL, FAX 35113953327

ABSTRACT

The Portuguese mainland coasts have been affected by strong earthquakes that generated tsunamis, destroying the city of Lisbon at least twice in the past (January 1531 and November 1755). The most significant known event is the Lisbon earthquake of the 1st November 1755, that generated waves 6 meter high in Lisbon and 30 meter high in Sagres (south Portuguese coast), as reported (Pereira de Sousa, 1909,1919). There are also historical reports of strong events that affected the Azores Islands, namely the events of 1522 at São Miguel, 1614 at Terceira, 1757 at São Jorge and 1837 at Graciosa.

The social and economic impact of an event like the 1755 earthquake is nowadays greatly amplified by the existent urban concentration near coastal areas. This fact emphasizes the importance of the spectral analysis of recent tsunamis recorded in the Portuguese coasts as a tool for predicting the interaction between tsunami waves with the main harbours and with populated coastal areas.

The 28th February 1969 earthquake, with magnitude $M_s = 7.3$, had its epicentre in the same tsunamigenic area of the 1755 event and an estimated focal depth of 22 km. The focal mechanism was determined by several authors e.g. McKenzie (1972), Udias (1972), Fukao (1973); the fault plane solution for this event is a thrust, with a small strike slip component, N55°E, parallel to Gorringe ridge (Fukao, 1973).

The 26th May 1975 earthquake, with magnitude $M_s = 7.9$, had its epicentre in the North Atlantic and an estimated focal depth of 15 km. The focal mechanism of this event accepted by several authors (Hirn et al, 1980), Lynnes and Ruff (1985), Grimson and Chen (1986), Buforn (1988) as an oceanic strike slip event.

In spite of the effective risk of tsunami waves this problem has attracted little attention in the past. The purpose of the present work is:

i) the numerical processing of the mareogram data available in order to infer accurate arrival times and tsunami amplitudes,

ii) the study of the spectral content of mareograms recorded in several tide gauge stations, determination of the spatial changes between stations and comparison of spectral content of the two events.

1. INTRODUCTION

The seismicity of the area, that is assumed as the seismogenetic location of the main events that affected the Portuguese coasts, is mainly controlled by the tectonic activity of Azores Gibraltar Fracture Zone (AGFZ), extending from the Azores towards the strait of Gibraltar.

Near the eastern end of this plate boundary, the Africa plate is presently underthrusting the european plate (Auzende et al., 1978) at an extremely low rate of 1-1.5cm/year (Purdy, 1975). This is a region of quite complex bathymetry, being the Gorringe Bank the most prominent topographic high (24 m depth, on the top of Gettysburg seamount). This bank, located north of the Azores Gibraltar plate boundary, is a structure of 200 km long and 80 km wide bounded to the south by the Horse Shoe Abyssal Plain (4500 m - 5000 m deep) and to the north by the Tagus Abyssal Plain (4500 - 5000 m deep).

Several models have been proposed to explain the genesis of this ridge and its strong gravity anomaly, with a maximum of +368 mgal, on the top of Gettysburg seamount (Bonnin, 1978). Some authors assume that the bank is a structure out of isostatic equilibrium, (e.g. Purdy (1975) and Le Pichon (in Souriau,1984), however Souriau proposed a model in which the bank is a structure isostatically balanced.

The hypothesis of Purdy and Le Pichon is compatible with the occurrence of strong earthquakes that might be tsunamigenic (magnitude > 6.0), but can not explain the reduced number of large events. It is possible that the existence of local low magnitude events, that dissipate energy gradually, may be a plausible explanation for the reduced number of large events recorded at the existent on-shore seismological network (Mendes Victor et al, 1991).

Several earthquakes with assumed epicentres in this area generated tsunamis in 60 BC, 382 AC (Galbis and Rodriguez in Campos (1989)), 1.11.1755 (Pereira de Sousa,1909,1919), 28.02.1969.

In the central zone, 25°W - 13°W, the AGFZ is an almost rectilinear fracture and its western end is known as the Gloria fault. This is an area of scattered seismicity.The epicentres show an east-west alignment, except for the 26 May 1975 event, which is located to the south of this alignment. The most important events located in this area are the 1939 event, M = 7.1 (Hirn et al., 1980), the 1941 event, M = 8.25 (Udias, et al., 1976) and the 26 May 1975, M = 7.9, Buforn (1988).

The western end of the AGFZ, in the vicinity of the Azores, between 35°W and 24°W, includes the triple junction of the American, European and Africa plates. The Mid Atlantic Ridge is crossed, to the north and to the south by east-west transform faults. In this area the seismicity is characterized by low magnitude but very frequent events. The predominant type of focal mechanism is normal or transform faults (Buforn,1988).

2. THE EARTHQUAKES OF FEBRUARY 1969 AND MAY 1975

The 28th February 1969 earthquake occurred at 2h40mn32.5s (TUC) and the epicentral coordinates, given by the USCGS, were 36.01°N, 10.57°W (Horse Shoe Abyssal Plain). The estimated focal depth was 22 km, being the mean water depth, over the epicentral zone, 4.5 km.

The focal mechanism of this earthquake has been determined by several authors (e.g. Udias (1972), Mckenzie (1972), Fukao (1973)); the fault plane solution is, according to Fukao (1973), a thrust with a small strike slip component, N55°E parallel to the Gorringe Bank (fig.1) and having an estimated seismic moment of $M_o = 6.0 \times 10^{20}$Nm. The fault dimensions, obtained through the analysis of the aftershock sequence, were 80 km long and 50 km wide.

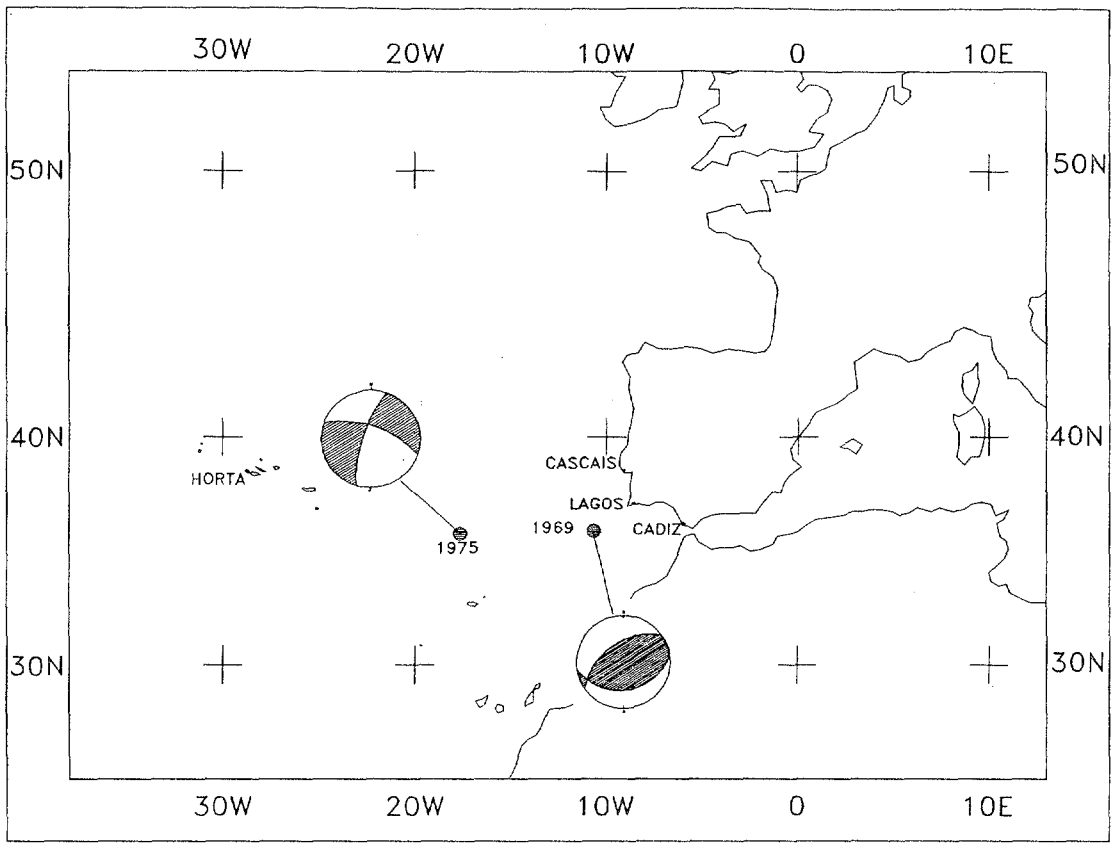

Figure 1 - Location of tide stations and focal mechanisms redrawn from:1969 event (Fukao, 1973); 1975 event (Buforn, 1988)

The earthquake of May 1975 occurred in the North Atlantic at 9h11mn51.3s (TUC) being the USGS epicentre coordinates 35.9°N, 17.6°W. The estimated focal depth was 15 km and the water depth over the epicentre area 5000 m.

According to Buforn (1988) this was an oceanic strike slip event, (fig.1), of magnitude $M_s = 7.9$ and seismic moment $M_o = 26 \times 10^{19}$ Nm. Hadley and Kanamori (1975) determined a similar focal mechanism and inferred a rupture of 150 km to NW. The same type of mechanism was accepted by Hirn et al.(1980), Lynnes and Ruff (1985) and Grimson and Chen (1986).

In spite of the agreement in the fault plane solutions proposed, Lynnes and Ruff (1985) pointed out some incoherences:

1. the value of the magnitude M_s is considered extremely high for an oceanic strike slip event;

2. this event generated a tsunami, clearly recorded at the Azores, Portugal mainland and Spain and this fact is compatible with a more significant dip-slip component; according to Ward(1980) and Comer(1982) the efficiency in generating tsunamis by strike slip events is about 1/3 of the efficiency of dip slip events, for equivalent seismic moment events. The same authors determined a different fault plane solution, based on Rayleigh wave data, with a larger dip-slip component.

3. SPECTRAL ANALYSIS OF MAREOGRAMS

3.1 Main conclusions from previous work

The application of spectral analysis to the interpretation of the tsunami records was done by several researchers (e.g. Munk et al., (1959, in Wiegel, 1964), Takahasi (1963, in Wiegel,1964), Loomis (1966), Miller (1972), Comer (1982), Abe and Ishii (1983), Soloviev and Kulikov (1987). The main conclusions of these works are the following:

- the form of tsunami spectra is strongly affected by local topography and by response functions of the harbours, where the tsunamis are recorded, varying significantly between stations for the same event; according to Munk et al. (1959) local resonance seems to be the controlling effect on tsunami spectra;
- although the response of a particular location is strongly dependent upon natural periods of oscillation, the peak energy occurs at different natural periods for different tsunamis, depending on the magnitude of the earthquake, (Takahasi, 1963); these spectral peaks obtained at different stations for the same event are explained by the influence of the "structure" of tsunami sources (Soloviev and Kulikov, 1987).
- amplitude spectral ratios were computed by Takasahi and Aida (1963, in Comer, 1982); they also averaged amplitude spectra from different tsunamis at a single tide gauge station to obtain a rough estimate of the transfer function of the station.
- according to Miller (1972) and Comer (1982) the variation of the spectra between stations due to the propagation paths, instrument effects and local resonances may be cancelled through the computation of ratios of spectra between different stations; this procedure permits the distinction between tsunami source effects and propagation + coastal interaction effects (Comer, 1982);
- the "effective tsunami period, T_e" is determined from the location of the maximum of tsunami amplitude spectra (or measured from peak to peak on tide gauge records); for a given water depth, in the generation region T_e is proportional to the predominant wavelength as $c=(gh)^{1/2}$; this parameter can be related to the square root of the source area and finally to the seismic moment, Comer (1982):

$$T_e \propto S_t$$
$$M_0 = \xi \Delta\sigma S^{3/2} \qquad (1)$$

where ξ is a dimensionless parameter depending on fault geometry, $\Delta\sigma$ is the stress drop and S is the fault area Aki (1972), S is considered approximately equal to the tsunami source area S

- the most important factor in determining the relative "colour" of a tsunami is, according to Miller (1972) the thickness of the water layer at the epicentre area as shallower water depth epicentre locations produce tsunamis relatively rich in low frequency energy;
- the shape of the spectra is also dependent upon seismic source dimensions and focal depth. Generally to shallower focus and large rupture dimensions correspond lower frequency tsunamis.

3.2 Methodology

The data used in this study was analyzed in four steps: digitization, interpolation, filtering and spectral analysis. Digitization was done from standard plots, using a digitizer tablet. The interpolation procedure consisted in a simple linear interpolation, between

sampled values, with sampling interval equal to 0.005 hour (18 seconds) (fig. 2). The separation of the tsunami signal from the tide record was then obtained using an high pass Butterworth filter, described bellow. Finally the spectra were estimated by the maximum entropy method of spectral analysis.

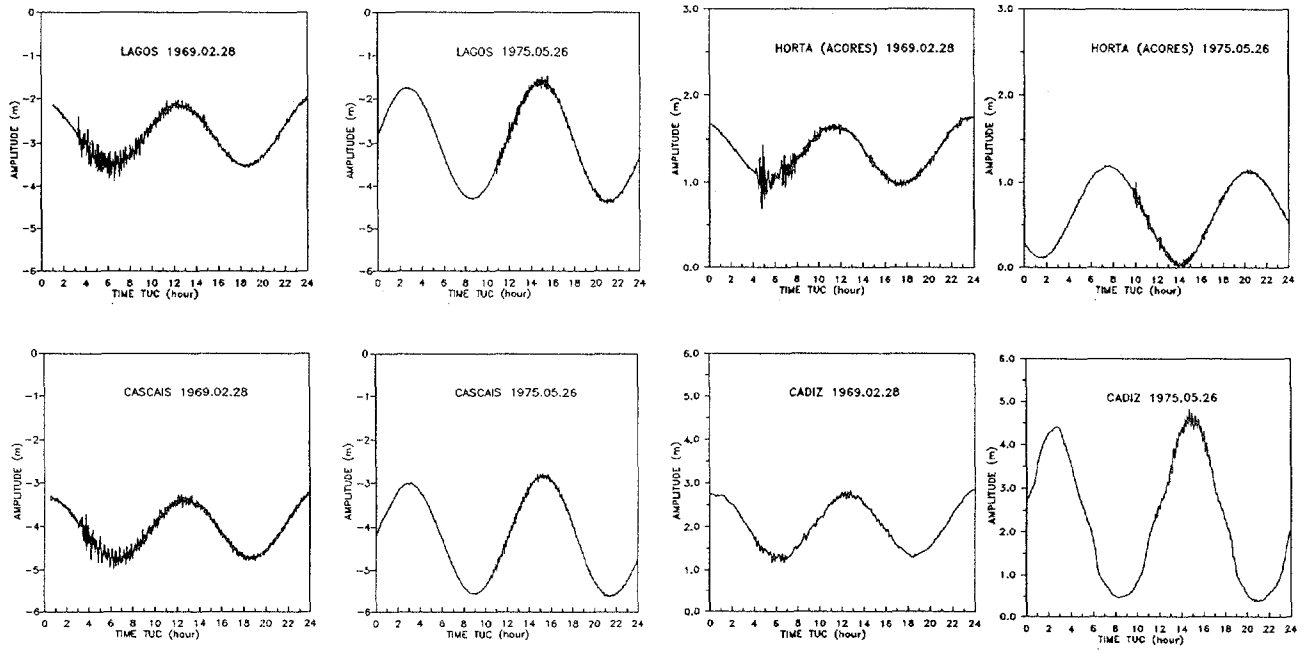

Figure 2 - Tide records

3.2.1 Filtering out the tide signal

The separation between the relatively short period tsunami oscillation and the much slower variation in sea height due to the tide, can be obtained with an high-pass filter properly designed. In the present study, we have decided to use a Butterworth filter, whose transfer function H is given by (Hamming, 1989):

$$|H(f)|^2 = 1 - \frac{1}{1+[\tan(\pi f)/w_c]^{2N}} \qquad (2)$$

The Butterworth filter is a recursive filter, which has a smooth transfer function highly adjustable through four parameters controlling its behaviour in both the pass and stop bands (ε and A) and the width of the transition band (f_s and f_p). Figure 3 shows the transfer function of the filter used, which corresponds to the values of $\varepsilon = 0.1$, $A = 10$, $f_s = 0.011$ min^{-1} and $f_p = 0.016$ min^{-1}, and Figure 4 shows the filtered tsunami signals.

3.2 Maximum entropy spectral analysis

The maximum entropy method (MEM) of spectral analysis, first introduced by Burg (1967), provides a powerful tool to estimate the power density spectrum of short time series, and of signals with superimposed noise. The theory underlying the maximum entropy method, which is closely related to Wiener's theory of optimum filters, can be found in several textbooks (e.g. Claerbout 1979). In the MEM the power density spectrum is

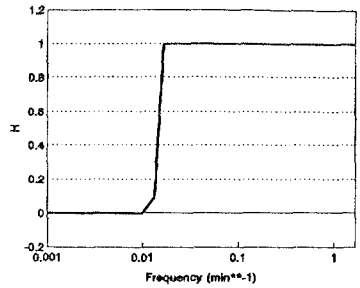

Figure 3 - Transfer function of the Butterworth high-pass filter

estimated as the inverse of the power density of the bilateral prediction error filter $(1,\gamma_1,...,\gamma_M)$:

$$P(f) = \frac{P_{M+1}\Delta t}{\left|1 + \sum_{k=1}^{M} \gamma_k e^{-2\pi i f k \Delta t}\right|^2} \qquad (3)$$

where M is the order of the filter, which must be imposed or determined by some external criterium, ...

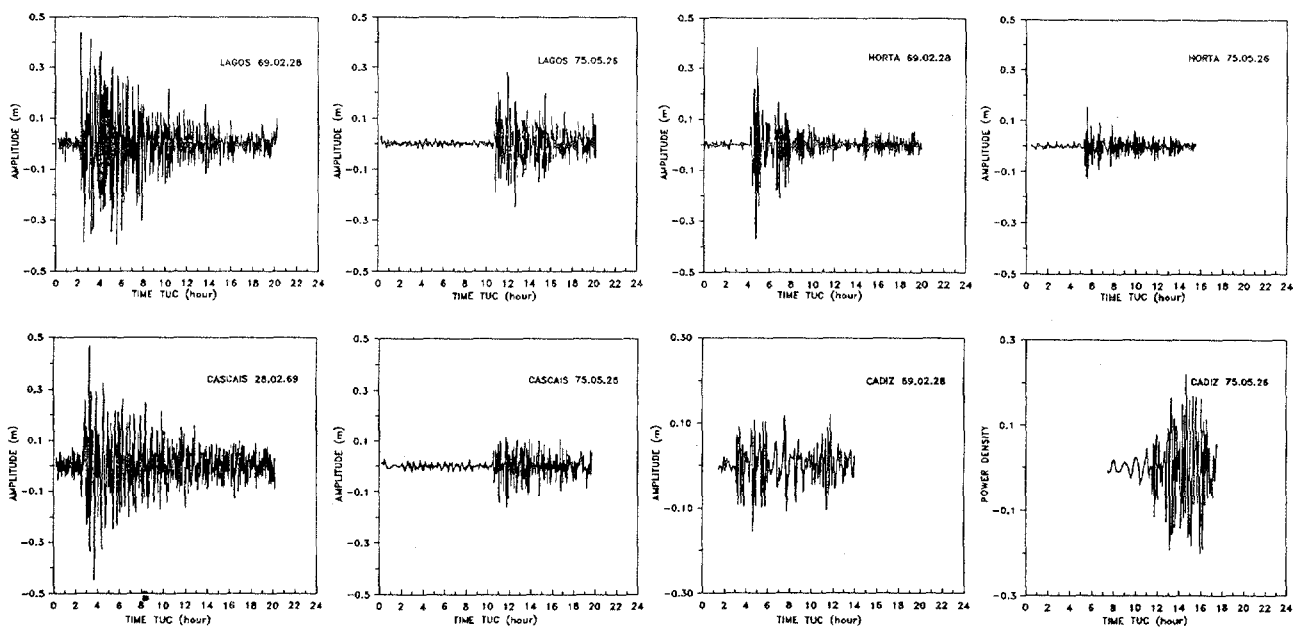

Figure 4 - Filtered tsunami signals

The definition of the number M is the critical aspect of this method. An increase in the value of M implies, in general, an increase in the spectral resolution but, at the same time, a decrease in the statistical significance of the estimate. In practice, most researchers will use some rule of thumb to define that number as a given fraction of the size of the sample being analyzed. In the present study, all spectra have being calculated with M = 100 (about 5% of the samples), which is a rather conservative choice. A few tests were made with significantly larger number of coefficients (up to M = 1000), showing little sensitivity of the method, in that range, in terms of the location of the main peaks of the spectra. On the other hand it is reassuring to note that the essential features of the MEM spectra are also present in the spectra obtained by straightforward Fourier analysis, which are, of course, much

noisier. A particular case is shown in Figure 9.

The evaluation of the prediction error filter implies an evaluation of the signal autocorrelation for different lags, up to the order of the filter. Burg (1967) algorithm admitted second order stationarity of the time series, resulting in a set of supersymmetric normal equations for the filter coefficients, efficiently solved by Levinson's recursion. In the present study, we use a generalization of Burg's method, developed by Barrodale and Erickson (1981), which does not assume the same degree of stationarity and which tends to offer an increase in spectral resolution, at the cost of increased computer time.

3.2.3 The deconvolution problem

The mareogram data consists of highly convoluted time series, where the tsunami signal is mixed with the properties of the medium where its propagation takes place, i.e., the ocean, coastal waters and the harbour or river estuaries. Assuming linearity, it is appropriate to use the theory of linear filters. The tsunami signal can be related to the mareogram by the convolution:

$$m(t)=z(t)*o(t)*c(t)*h(t) \tag{4}$$

where z(t) is the tsunami signal and o(t), c(t) and h(t), the impulse response functions of the deep ocean, the coastal waters and the harbour. In the spectral domain, the relation expressed by the + previous equation is a lot simpler, because the operation of convolution is replaced by a simple product (this is the convolution theorem of Fourier analysis). That is the essential reason to use spectral methods in the analysis of this data. We have then:

$$M(\omega)=Z(\omega)O(\omega)C(\omega)H(\omega) \tag{5}$$

If the propagation is a strongly non linear process the meaning of the spectra of mareograms is unclear. In spite of that, it is reasonable to believe that the linear analysis will provide relevant information for both linear and weakly non-linear cases. According to Comer (1982) the propagation path and instrument effects taken together, should behave like a time invariant linear filter, unless the amplitude grows too large as the water shallows before it reaches the tide gauge, which is not the case of the events we present in this study; assuming that propagation and instrument effects act like a linear filter, the tsunami near its source corresponds to the input signal and the mareogram record is the output signal.

In the present study we consider mareogram data at four different locations: Cascais and Lagos at the portuguese mainland west and south-west coasts, Cadiz (Spain) and Horta (Azores Archipelago), covering a large azimuthal range (cf. fig 1). In each location, spectra for the two tsunamis (February 1969 and May 1975) were calculated, together with spectra for tsunami-free days (quiet-days) in two of the locations, where appropriate data was available. Comparing those spectra it is possible to use relations (4-5) to infer some information about the different terms on the right hand side. At the same location, H(ω) is always the same, whereas Z(ω) will depend on the event being analyzed. On the other hand O(w) and, possibly, C(ω) depend only on the location of the perturbation source.

4. RESULTS

4.1 The Tsunamis of February 1969 and May 1975

The earthquakes of February 1969 and May 1975 generated small tsunamis that were clearly recorded at the Portuguese mainland tidal network, in some Spanish places, in Morocco and in the archipelagos of Açores e Madeira. Abe (1979), based on tsunami height reported values, used this event to attribute the value 8.6 to the tsunami magnitude (M_t) of the 1st November 1755 Lisbon earthquake.

Once isolated the tsunami signal the travel time and maximum amplitude of the sea waves can be accurately calculated from the digital records obtained. These values are listed in the table below, the amplitude range correspond to: (maximum amplitude - minimum amplitude).The following table presents a summary of data obtained at Cascais, Lagos, Horta and Cadiz.

STATION	LOCATION	TRAVEL TIME (mn)	AMPLITUDE (cm)	1st MOV	T_e (mn)
CASCAIS 69	38°41'N 08°24'W	37.0	93.2	UPWARD	19.2
CASCAIS 75	38°41'N 08°24'W	83.6	27.4	UPWARD	13.5
LAGOS 69	37°05'N 08°39'W	35.5	84.3	UPWARD	14.4
LAGOS 75	37°05'N 08°39'W	90.1	53.1	UPWARD	7.4
HORTA 69	38°32'N 28°37'W	90.3	75.5	UPWARD	15.3
HORTA 75	38°32'N 28°37'W	33.9	28.3	DOWNWARD	10.5
CADIZ 69	36°28'N 06°15'W	84.0	28.4	DOWNWARD	16.4
CADIZ 75	36°28'N 06°15'W	143.0	21.5	UPWARD	12.7

The average effective periods were determined from the location of the strongest peak in the power density spectra, the predominant wavelengths in the generating regions were obtained assuming the following values for the water depth at the epicentre regions: $h_{69} = 4500$ m and $h_{75} = 5000$ m:

$$\begin{aligned} T_{e(69)} &\simeq 16mn \Rightarrow \lambda_{p(69)} \simeq 200km \\ T_{e(75)} &\simeq 11mn \Rightarrow \lambda_{p(75)} \simeq 150km \end{aligned} \qquad (6)$$

4.2 Analysis of Tsunami Spectra and discussion

The investigation of harbour effects and the comparison of tsunami source effect through the procedure described in section 3.2.3 and used by Miller (1972), Comer (1982) can not be applied in our study due to the difference in epicentre location. The calculation of amplitude spectral ratios in order to cancel station response implies that the terms, in equation 5, $O_{69}(\omega)$ and $O_{75}(\omega)$ must be coincident. The strong dependency of those terms on the location of the perturbation source does not allow the comparison of tsunami signals through the ratio: $Z_{69}(\omega)/Z_{75}(\omega)$.

The existent tidal network is sparse and the stations with coincident propagation paths are those located along the Tagus Estuary (Lisbon). Furthermore, for those events

mareogram data is only available in one station (Terreiro do Paço). Although the distance between this station and Cascais is less than 30 km the spectra obtained at Terreiro do Paço incorporates the effects of the propagation along the estuary, where strong non linear effects may become too important to permit a reliable comparison of tsunami source effects.

The methodology described in section 3.2.1 and 3.2.2 was applied to the records of the following days: the day before the earthquake, the day of the earthquake and the day after the earthquake. The objective of this procedure was the establishment of the spectral characteristics of the tidal records in the absence of a tsunami and the comparison between tsunami-day-record/quiet-day-record.

Due to the poor quality of the 1969 available records we have been able to digitize only the record of 28.02.1969 in Lagos and Cascais and the record of 27.02.1969 in Lagos. The quality of the 1975 records allowed the digitization of the days 25, 26 and 27 May in both stations. From the station in the Azores (Horta) we digitized only the days of the earthquakes.

The first conclusion can be deduced through the analysis of the "quiet days" spectra (cf. fig.5), the spectrum of each station presents quite well defined peaks that should correspond to the "bathymetric signature" of the harbours.

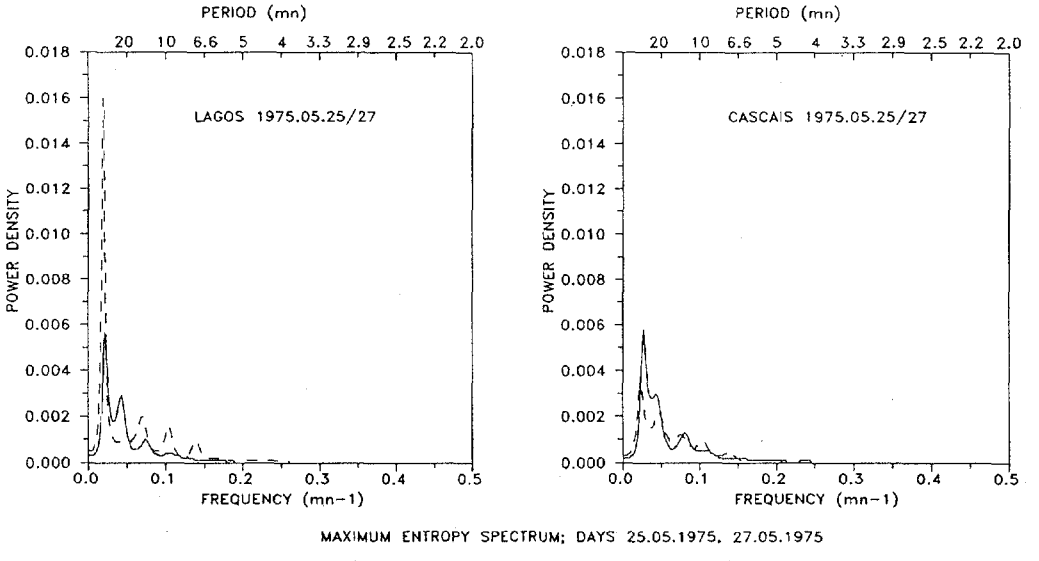

Figure 5 - Maximum Entropy Spectrum of the "quiet" days of 25/27 May 1975; (25 May - dashed line; 27 May solid line)

From the analysis of figure 6 corresponding to the comparison, at Cascais and Lagos, "quiet-days"/"tsunami-days", it seems that the occurrence of a tsunami does not change, significantly, the peaks observed in quiet days spectra, although their amplitudes are clearly amplified. This result is valid for both stations and for both tsunamis.

The third conclusion is that different tsunami signals recorded at the same station amplify different peaks, from the analysis of Figure 7 we could say that the 1969 event is "more-red" and the 1975 event is "more-blue". This result is in good agreement with the source parameters referred in section 2 as we should expect more high frequency radiation from the 1975 event (focal depth 15 km) than from the 1969 event (focal depth 22 km). The smaller amplitudes in the power density spectra of the 1975 are also consistent with the fact that the strike-slip mechanism is substantially less efficient for tsunami generation than dip-slip events, in spite of the difference in seismic moments.

Through the analysis of Figure 8 we can say that the main energy of the 1969 event lies in the period range of (6-37) mn with an apparent maximum around 14 mn; this value

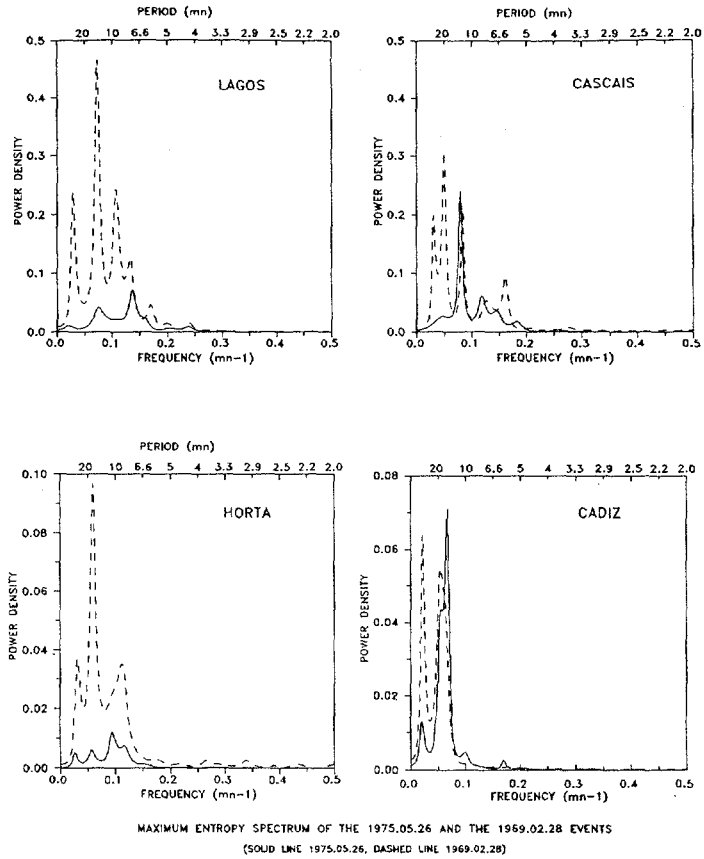

Figure 6 - Maximum Entropy Spectrum of the 1969 and 1975 events
Solid line: 1975.05.25; Dashed line: 1969.02.28

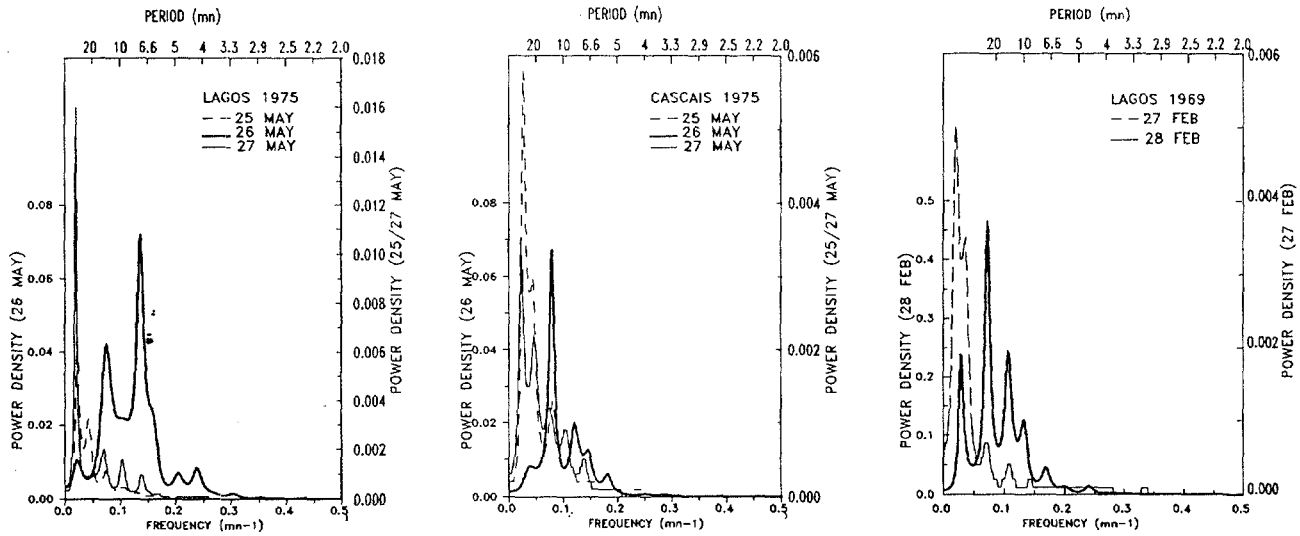

Figure 7 - Comparison between the spectra in "quiet" and tsunami-days

is not significantly different from the average effective period determined (16 mn). Figure 9, presents a comparison between the MEM power density spectrum and the Fourier spectrum, showing good consistency and, at the same time, the advantage of the method used in this study. On the other hand it should be noted that the period naively measured on the mareogram from the distance between sucessive peaks, shows a significant change with

time, as a result of wave dispersion. This could lead to errors in the evaluation of the effective period and shows the necessity of the use of spectral analysis methods.

The energy distribution of the 1975 event is quite different and it seems to split in a "bi-modal" way: (4-8) mn and (8-46) mn. This fact and the influence of different focal mechanisms of the two events certainly deserves a more detailed analysis that goes beyond the scope of the present study.

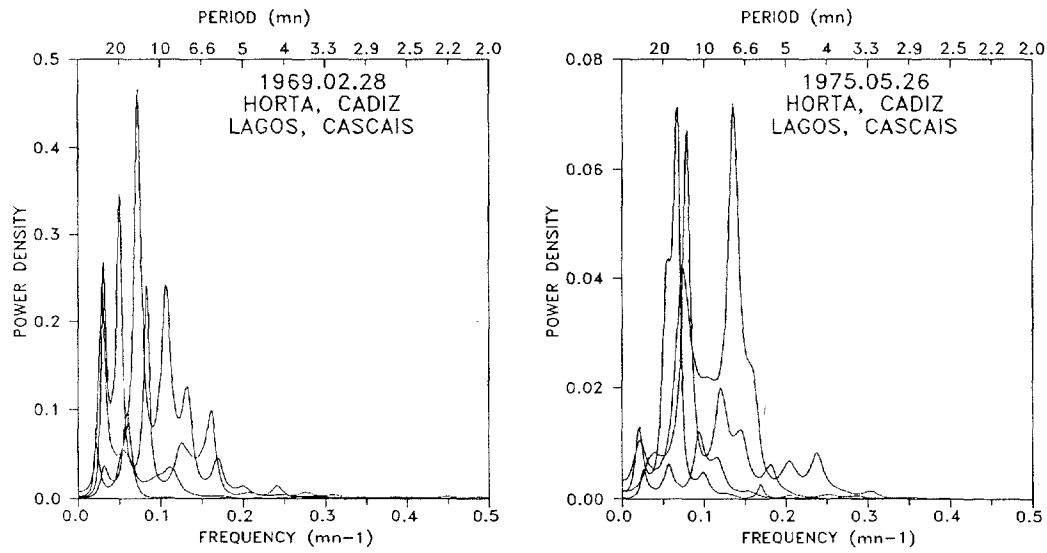

Figure 8 - Overlapping spectra (m.e.m.) from different stations for the 1969 (left) and the 1975 (right) events.

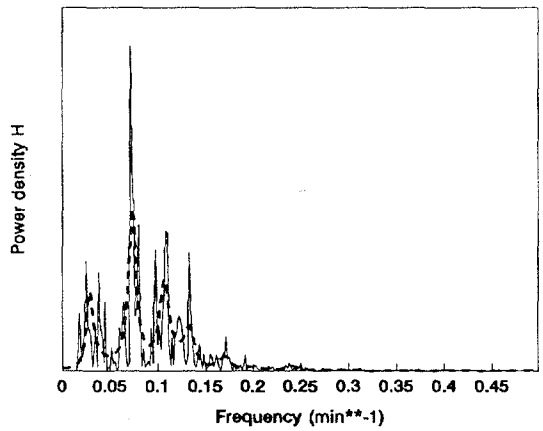

Figure 9 - Comparison between MEM (dashed line) and Fourier (full line) spectra (Lagos 1969)

ACKNOWLEDGMENTS

The authors acknowledge gratefully the contributions from the following institutions and persons: Instituto Geográfico e Cadastral (Lisboa), Eng. José Formosinho, Professor Lourdes Campos from Universidad de Castilla-La-Mancha, and Junta Autónoma dos Portos de Angra Heroísmo.

REFERENCES

Abe K., 1979. Size of great earthquakes 1873-1974 inferred from tsunami data. J. Geophys. Res., 84, 1561-1568.

Abe K., Ishii H., 1983. Study of shelf effect for tsunami using spectral analysis. In: Tsunamis - their science and engineering, ed. by K.Iida and T Iwasaki, Tokio, TERRAPUB, 161-172.

Aki K., 1972. Earthquake mechanism. Tectonophysics, 13, 423-466.

Auzende J.M., Olivet J., Charvet J., Le Lann A., Le Pichon X., Monteiro J., Nicolas A., Ribeiro A., 1978. Sampling and observation of oceanic mantle and crust on Gorringe Bank. Nature, vol. 273, pp 45-48.

Barrodale I., Erickson R.E., 1980. Algorithms for least squares linear prediction and maximum entropy spectral analysis. Geophysics, 45, 420-446.

Bonnin J., 1978. Évolution géodynamique de la ligne Açores-Gibraltar.Thèse presentée à l'Université Pierre et Marie Curie, Paris VII.

Buforn E., Udias A., Colombas M., 1988. Seismicity source of the mechanisms and tectonics of the Azores-Gibraltar plate boundary. Tectonophysics, 152, 89-118.

Burg J.P., 1967. Maximum entropy spectral analysis. Presented at the 37th Annual International SEG Meeting, Oklahoma City, Oklahoma, October 31, 1967.

Campos M.L., 1991. Tsunami hazard on the Spanish coasts of the Iberian Peninsula. Science of tsunami hazards, vol.9, n°1, pp 83-90.

Claerbout J., 1976. Fundamentals of geophysical data processing. McGraw Hill, N.Y.

Comer R., (1982) Tsunami generation by earthquakes. Phd thesis, Massachusetts Institute of Technology.

Fukao Y., 1973. Thrust faulting at a lithosphere plate boundary. The Portugal earthquake of 1969. Earth and Planet. Sci. Lett., 18, 205-216.

Grimson N.L., Chen W., 1986. The Azores Gibraltar plate boundary: focal mechanisms, depths of earthquakes and their tectonics implications. J. Geophys. Res., 92, 2029-2047.

Hadley D.M., Kanamori H., 1975. Seismotectonics of the eastern Azores-Gibraltar ridge. (Abstract), EOS, 56, 1028.

Hamming, 1989. Digital filters. 2nd ed. Elsevier.

Loomis H.G., 1966. Spectral analysis of tsunami records from stations in the Hawaiian Islands. Bull. Seism. Soc. Am., 56, 697-713.

Lynnes C.S., Ruff L.J., 1985. Source process and tectonic implications of the great 1975 North Atlantic earthquake. Geophys. J. R. Astr. Soc., 82, 497-510.

Mckenzie D., 1972. Active tectonics of the Mediterranean region. Nature, vol. 226, pp 229-243.

Mendes Victor L., Baptista M.A., Simões J., 1991. Destructive earthquakes and tsunami warning system. Terra Nova, vol.2.3.

Miller G., 1972. Relative Spectra of Tsunamis. Hawaii Institute of Geophysics, HIG-72-8, University of Hawaii, Honolulu.

Pereira de Sousa F.L., 1909. Effeitos do terramoto de 1755 nas construcções de Lisboa. Lisboa 1909.

Pereira de Sousa F.L., 1919. O terramoto do primeiro de Novembro de 1755 em Portugal e um estudo demográfico. Lisboa, 1919.

Purdy G., 1975. The eastern end of the Azores Gibraltar plate boundary. Geophys. J.R.Astr. Soc., 43, pp 973-1000.

Soloviev S., Kulikov E., 1987. Spectral analysis of mareograms from Urup tsunamis of 13 and 20 October 1963. Science of tsunami hazards, vol.5, n°1, pp 57-63.

Souriau A., 1984. Geoid anomalies over Gorringe ridge , north Atlantic, Earth and Planet. Sci. Lett., 68, pp 101-104.

Udias A., Arroyo A., 1972. Aftershock sequence and focal parameters of the February 28, 1969 earthquake of the Azores Gibraltar fracture zone. Bull. Seism. Soc. Am., pp 699-719.

Ward S., 1980. Relationships of tsunami generation and an earthquake source. J. Phys. Earth, 28, 441-474.

Wiegel R., 1964. Oceanographical Engineering, 95pp.

TSUNAMI GENERATED FORMS IN THE ALGARVE BARRIER ISLANDS (SOUTH PORTUGAL)

C. **Andrade** (Departamento de Geologia, Universidade de Lisboa)

ABSTRACT

"Ria Formosa" is a small barrier island system of central and eastern Algarve (south Portugal), a mixed energy, tide dominated and medium energy coast.

Incorporation of washovers, dune, beach or curved spit ridges and tidal deposits, near barrier tips, account for most of the accretionary deposits and forms observed in the backbarrier areas.

The tsunami generated by the megaseism of Lisbon (1 November 1755) severely damaged the barrier chain, leading to the drawning and amputation of its oriental extremity and to the extensive overwash of two of the eastern barrier islands (Armona and Tavira).

Analysis of the morphology of these islands strongly suggests that their backbarrier areas preserve depositional features generated both by the massive injection of sands through the former barrier and by a fast reorganization of the tidal drainage system, following the overwash event.

These processes were completed later by the differentiation of a beach - foredune structure, still active today, supported by a second generation of small, coalescent overwash fans, that partially outcrop on the lee side of the foredune.

Once established, this outer structure would seal the inner barrier surface, inhibiting further cross-shore exchanges with the open ocean, leaving a strongly dissected surface available for tidal creek remodelation. Actually, the organization of the backbarrier tidal network seems to be directly inherited from the drainage reorganization event afore-mentioned.

1. Introduction

The "Ria Formosa" barrier system is a small barrier island chain and associated lagoon that forms the dominant physiographic unit of the central and eastern coast of Algarve (south Portugal), extending from the region of Quarteira to the Guadiana estuary, along aproximately 55 Km (Fig. 1).

The system is roughly triangular in shape, elongated towards northeast and near Cape Sta. Maria the barrier attains its maximum distance from mainland: aproximately 6 Km.

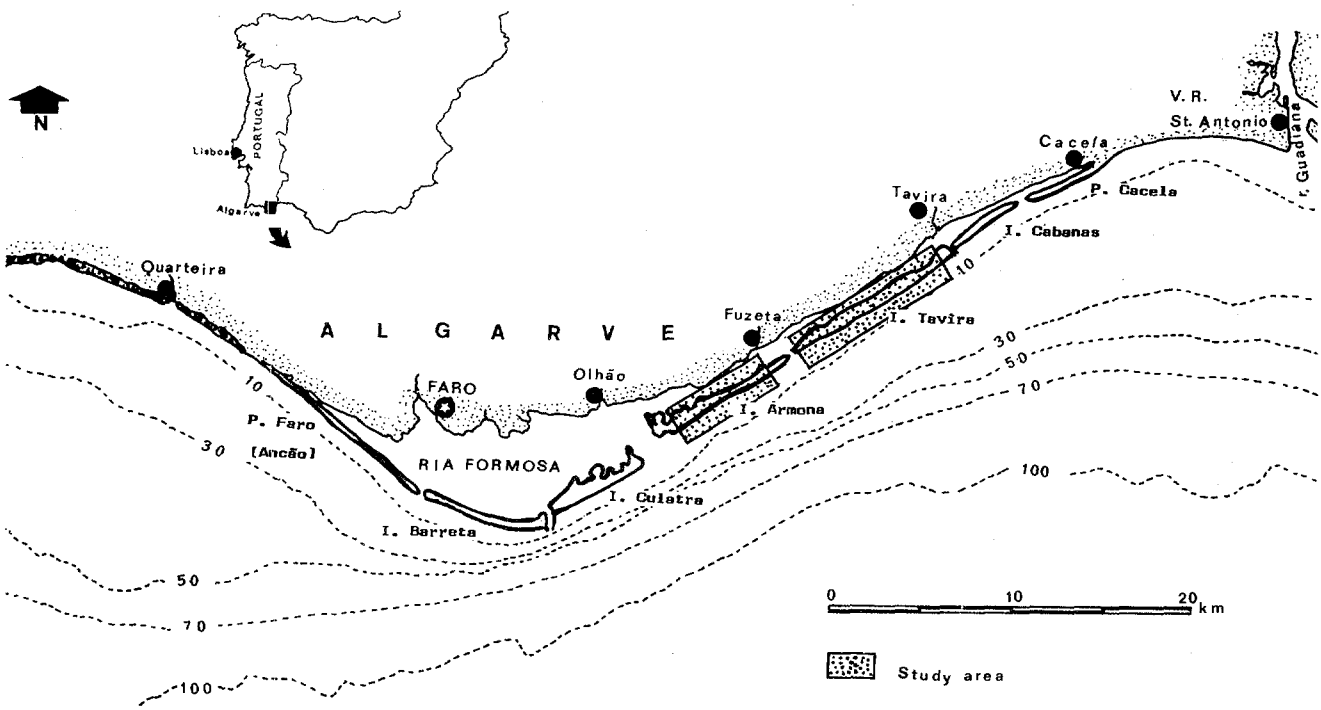

Fig. 1 - Location map and study area

The southern coast of Portugal is high mesotidal, according to Hayes (1979). Tides are semidiurnal and maximum tidal range may occasionally exceed 4m (aproximately 1% of the year).

Wave climate is of medium energy (classification of Hayes, 1979), strongly influenced by short period sea (see Pessanha e Pires, 1981 or Pires e Pessanha, 1979 for details). Average significant wave height and period are small (0.9 m and 5 s, repectivelly), and calm sea is recorded during 25% - 30% of the year. This mild regime is occasionally disrupted by storms associated to the octants of southeast or southwest. Extreme southwesterns may be very damaging to the coast and are typically short-lived (2 to 4 days): recorded mean values of Hs of 4 m are usual, but 6 m is exceptional (recurrence lag of about 50 years).

Storm-generated overwash deposits are common features on the barriers. However, the relative importance of overwash in the cross shore sand budget of the barrier chain is poorly known. Pilkey et al. (1989) stressed the importance of washovers both as morphology-building units and as sediment traps. More recently Andrade (1990, 1991) showed that overwash is not a dominant process of sediment transfer and that correlated deposits occur almost entirely concen-

trated in recently accreted barrier tips. Further consolidation of the barrier includes the settling of embrio foredunes which compete with washovers for the occupation of the supratidal area of the barrier. In a few years aeolian structures consolidate, spread and coalesce, sealing the low-lying backbarrier surface except in very localized sites where chronical overwash may persist for longer periods.

Washovers are essentially represented by single, discrete, elongated drop-shaped structures,similar to the breach-throat-fan splays quoted by Carter (1988), that seldom cross the whole backbarrier flat (less than 20% of the observed features on the ocean-facing margin of the barriers). Figure 2 presents a typical example of storm generated washover distribution in one of the eastern and more recent (less than 100 years) barriers. Historical records and field evidence clearly show that even the most damaging storms recorded in this century fail to "behead" the islands extensively. Instead, the resulting topography is better characterized by the multiplication os small deposits, rarelly coalescent, alternating with a discontinous foredune ridge, defining a morphology roughly correspondent to types III-IV of Hesp's (1988) classification.

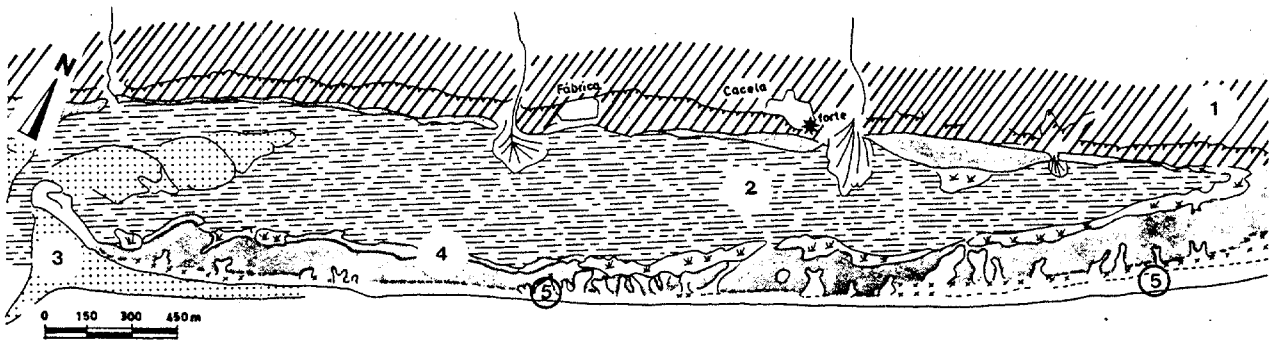

Fig. 2 - Washover pattern at Cacela peninsula, after Andrade (1991).
1 - Mainland; **2** - Lagoonal flats; **3** - Tidal delta deposits; **4** - Backbarrier surface, marginal marsh and foredunes; **5** - Beach and washover lobes.

With exception of the study area the general morphological framework of the islands backbarrier is dominated by the incorporation of forms related with rapid drifting of tidal inlets and consequent barrier-tip extention or enlargement: recurved spits, beach ridges and abandoned segments of tidal deltas are common examples (Fig. 9).

The barrier chain is receeding, mainly because of sediment starvation, though some authors also suggested adjustment to a rising sea-level as another cause for barrier recession (e.g. Pilkey et al, 1989; Andrade, 1991). Recent (last 300 years) changes in the global geometry of the system affected essentially the eastern and western edges. Maps and written documents clearly show that deactivation, silting and obliteration of two terminal inlets induced the welding of former islands to mainland leading to the differentiation of the actual extreme peninsulas of Ancão and Cacela. Starvation of the central barriers seems to activate an almost pure erosive process, rather than rollover or barrier translation.

2. Seismicity, tsunamis and coastal change

Most large magnitude, historical earthquakes recorded in Portugal have their epicentral areas associated to the intraoceanic subduction zone located immediatly south of the Gorringe Bank (Ribeiro et al, 1979), a segment of a larger structure that extends from the Açores until

the eastern Mediterranean (Fig 3).

The most destructive event, associated to vertical displacement of the sea-floor, ocurred in 1 November 1755. This shallow focus seism had an estimated magnitude of 8.5-9 (maximum intensity X-XI under MS scale) and triggered a large tsunami that hit the whole western and southern Portuguese coast as well as the Spanish southern shoreline until Algeciras, west of Gibraltar (Romero, 1989).

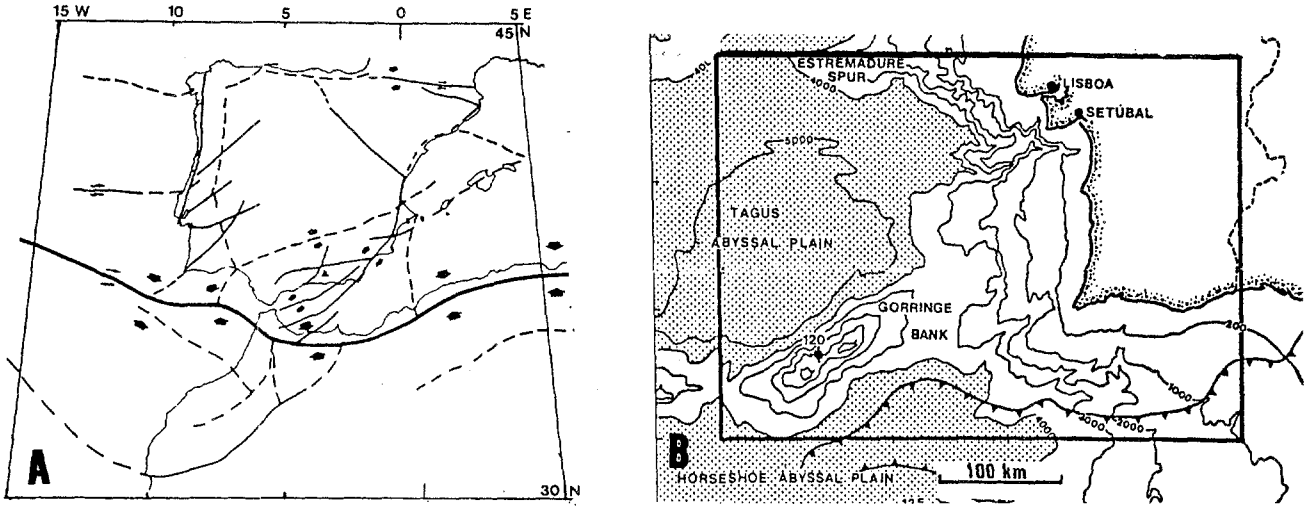

Fig. 3 - (**A**) General seismotectonic sketch of the Açores-Gibraltar area (adapted from Romero, 1989)and (**B**) location of Gorringe Bank (adapted from Mougenot, 1988).

The first tsunami wave arrived at the Algarve at low tide and was followed by several (Romero, 1989 reports 18) secondary waves. Spanish information about wave height on arrival at Cadiz (compiled by Romero, 1989 and variable between 11 m and 20 m) may not be extrapolated elsewhere, because of local geometric effects induced by the Cadiz bay plan shape and bathymetry. However, available records of damage suffered by the Algarve west coast and an eyewittness account of the overwash of Ancão peninsula (western barrier of Ria Formosa lagoon) described by Pereira de Sousa (1919-1932) suggest that a figure of 9 m is a plausible minimum.

Estimated wave height is quite enough to produce extensive overwash of the whole barrier and disruption of the former chain, leading to catastrophical change in coastal physiography. Cartography clearly shows that this was the case at the oriental tip of the former barrier chain. The easternmost part of Tavira island, that originaly extended until the Guadiana estuary, was destroyed and reformed later, but welded to mainland, constituting the actual coastal plain of Manta Rota.

Two maps, dated from 1762 (Carpinetti Lisbonense and Rizzi Zannonni, one of which is represented in Fig. 4), also show a unique, unexpected and very interesting representation of Tavira and Armona islands: their central areas are explicitely shown as intertidal, a representation that is never found in doccuments produced later than 1765 or earlier than 1755. Also, the location of this intertidal and consequently open inlet area is not expectable, according to the tidal prism-inlet relashionships that have been derived for this particular sector of the barrier system by Andrade (1991), sugesting that it corresponds to an instantaneous picture of coastal healing, developed after a major destructive event.

Morphological analysys of the backbarrier surface of these two islands reveals a unique pattern, compatible with the exceptional overwash event and with the drainage network reorganization process that must have followed the 1755 tsunami.

Fig. 4 - Partial reproduction of C. Lisbonense's map, showing the eastern islands of Ria Formosa as intertidal shoals.

3. The study area

Within the study area the inner lagoon is very shallow, narrow and elongated alongshore (Fig. 5). Tidal waters are conveyed by one main axial channel from which several radial tributaries emanate, nourishing a bare mudflat margined by a vegetated high saltmarsh platform (aproximated elevation 3.0-3.5 m-H.Z.). The marsh confines with the barrier by a marked step, sometimes scarped (Fig. 6).

The backbarrier surface is made of a sandy, sparsely vegetated platform (elevation 4-4.5 m - H.Z.) dissected by a labyrinthic, second order channel network. These wide and very shallow channels outline an almost chaotic field of vegetated sand mounds, very irregular in plan shape that seem randomly dispersed, when viewed from the ground (Fig. 7). Channel bottom sands may be reactivated in spring tides by flood-dominated currents (Fig. 7) and mound slopes respond to water-level carving during flood events, through vegetation killing and small scale avalanching (Fig. 8). These processes slowly nibble and dilute the backbarrier relief, nourish channel floors and allow the redistribution of sand through the backbarrier area, without significant excavation of thalveg lines.

Viewed from the air (Fig. 8) the backbarrier surface has a definitely organized morphological pattern, controled by repetitive, radial, first order channels. They are tributaries to the main axial channel, and embrace several ovoid segments of surface, their incision rate increasing away from the outer margin of the barrier. A first order channel typically terminates against the lee side of the foredune by a dead-end, where course, iron-stained clastic lags may be found paving the surface or buried beneath an incipient marginal marsh deposit, whose growth is promoted by floodwater ponding. Hydraulic connection between a pair of consecutive first order channels is ensured in spring waters by the second order network afore-mentioned.

First order channel heads occurr closely associated to or margined by single or multiple curved or bended linear sand ridges, that emerge out of the downwind slope of the foredune. These are interpreted as relict recurved spits, similar in shape, dimensions and position to their active counterparts of the same barrier chain: they margin the main channel of fast-drifting tidal inlets, near the inlet gorge, or the vestibular area facing the flood ramp, close to the bifurcation point of the peripheral channel that cicunscribes the flood delta (see Andrade, 1991 for details).

Actually, the large ovoid surface segments of the backbarrier area present a striking similarity in shape, dimensions and internal architecture with the flood structures of small and unstable (mobile) inlets of the same barrier system. Fig. 9 presents an example from Fuzeta inlet.

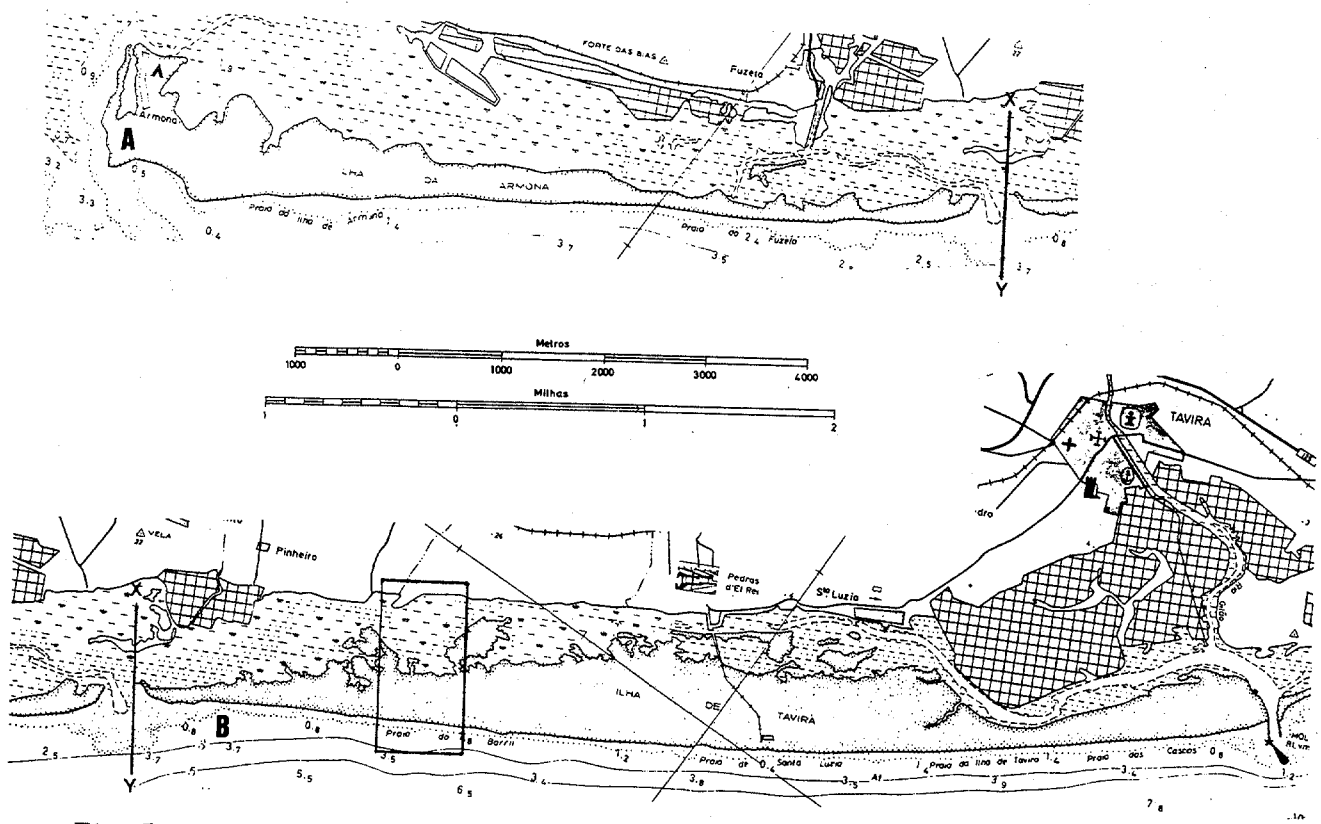

Fig. 5 - Armona (**A**) and Tavira (**B**) barriers, showing the elongated inner lagoon. Squared area in B shown in detail in fig. 9.

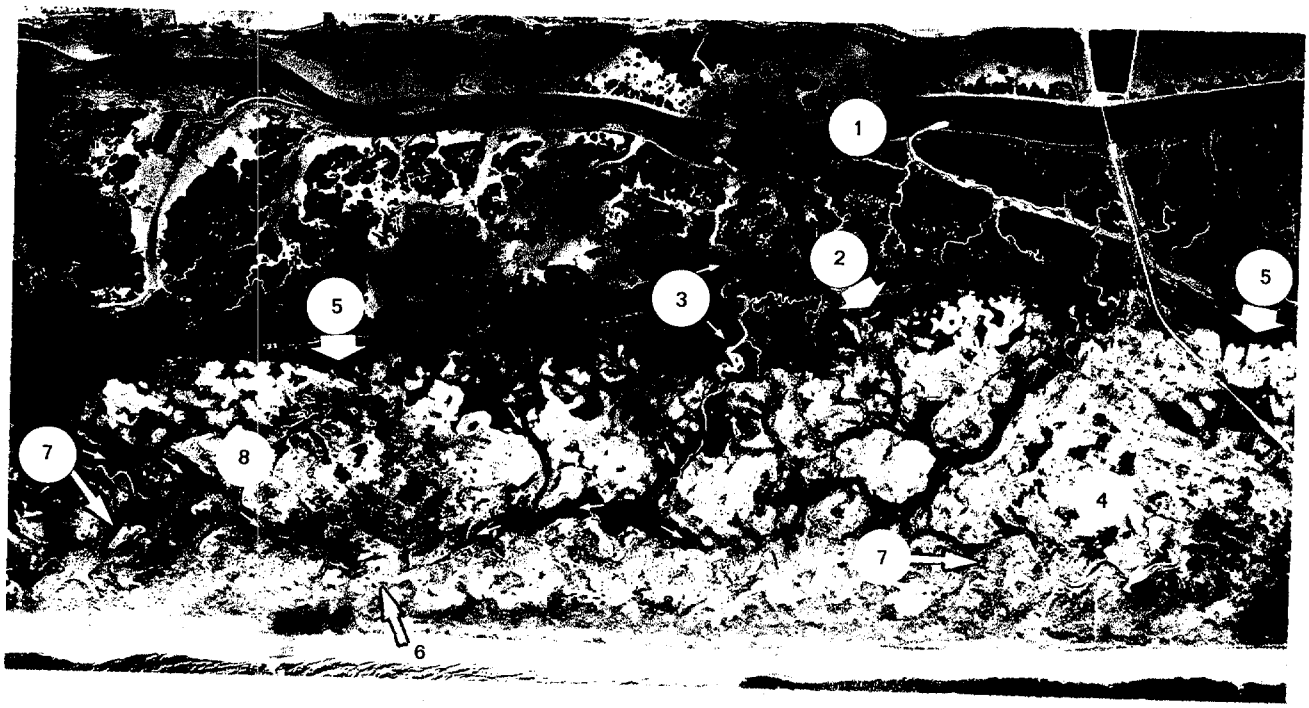

Fig. 6 - Vertical photography (1:15000, FAP-1984) of central part of Tavira Island. **1** - main channel; **2** - marsh; **3** - first-order, radial channel (small arrows); **4** - second order channels on backbarrier surface; **5** - ovoid, relict tidal deltas; **6** - dead end: second-order channel head; **7** - relict recurved spits emerging out of the foredune; **8** - abandoned lobe of flood delta.

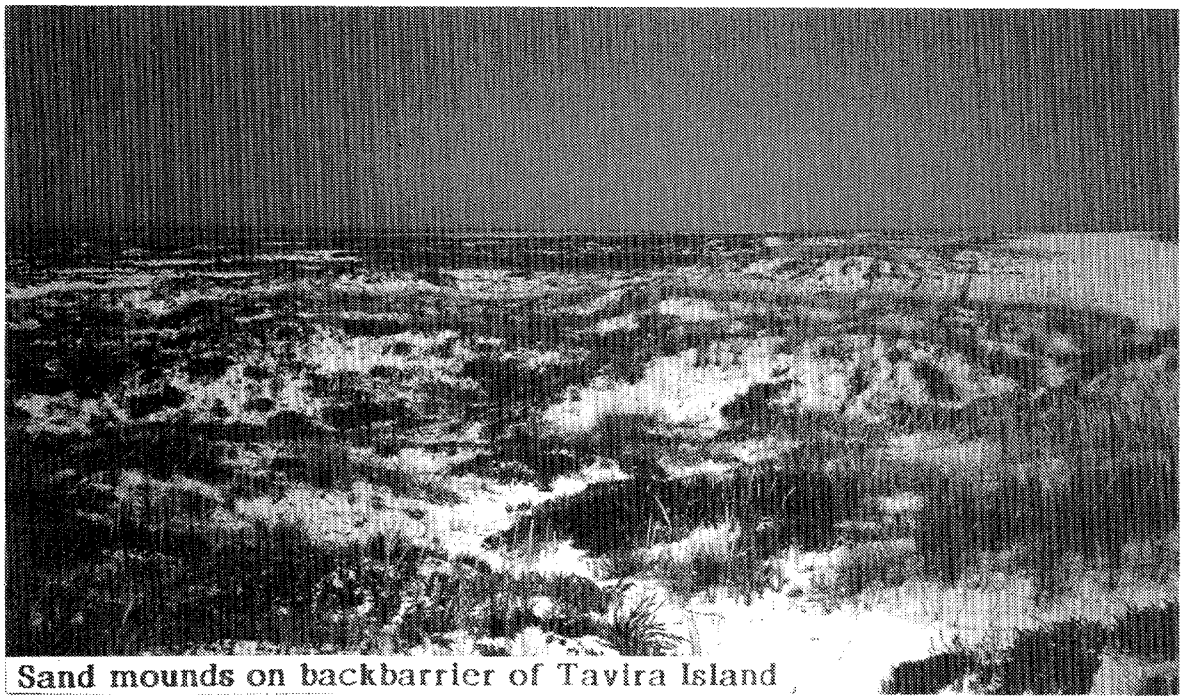

Sand mounds on backbarrier of Tavira Island

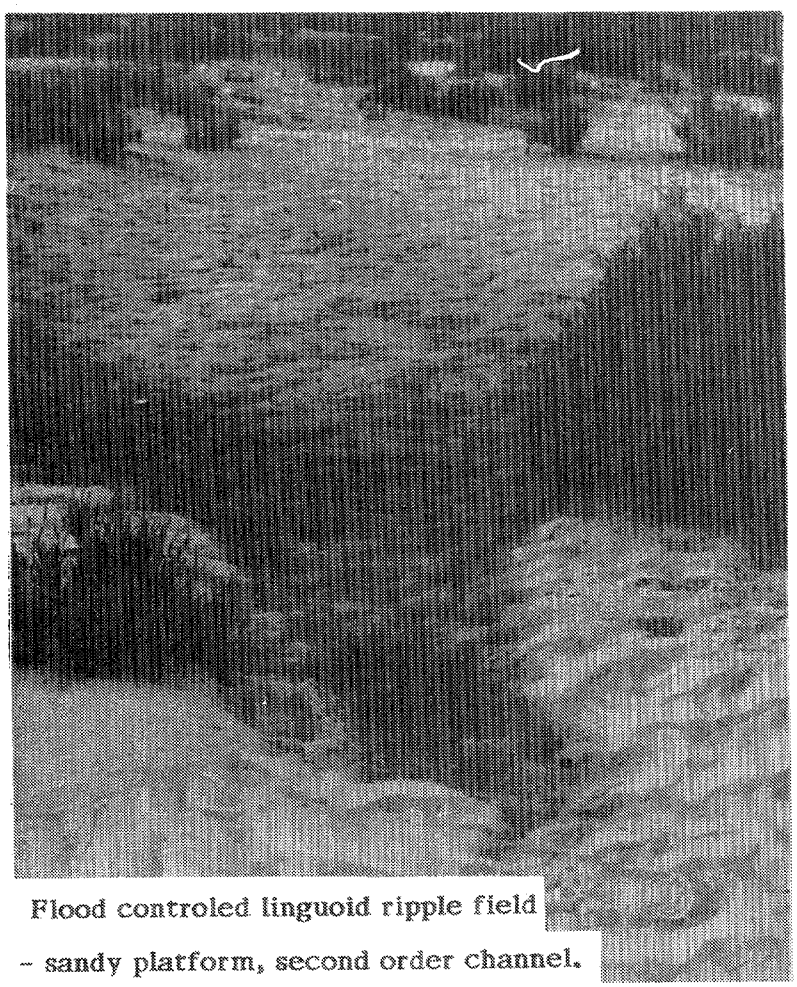

Flood controled linguoid ripple field - sandy platform, second order channel.

Fig.7
Ground view of Tavira island backbarrier hummocky surface (above) and reactivation ripple field on second-order channel (left).

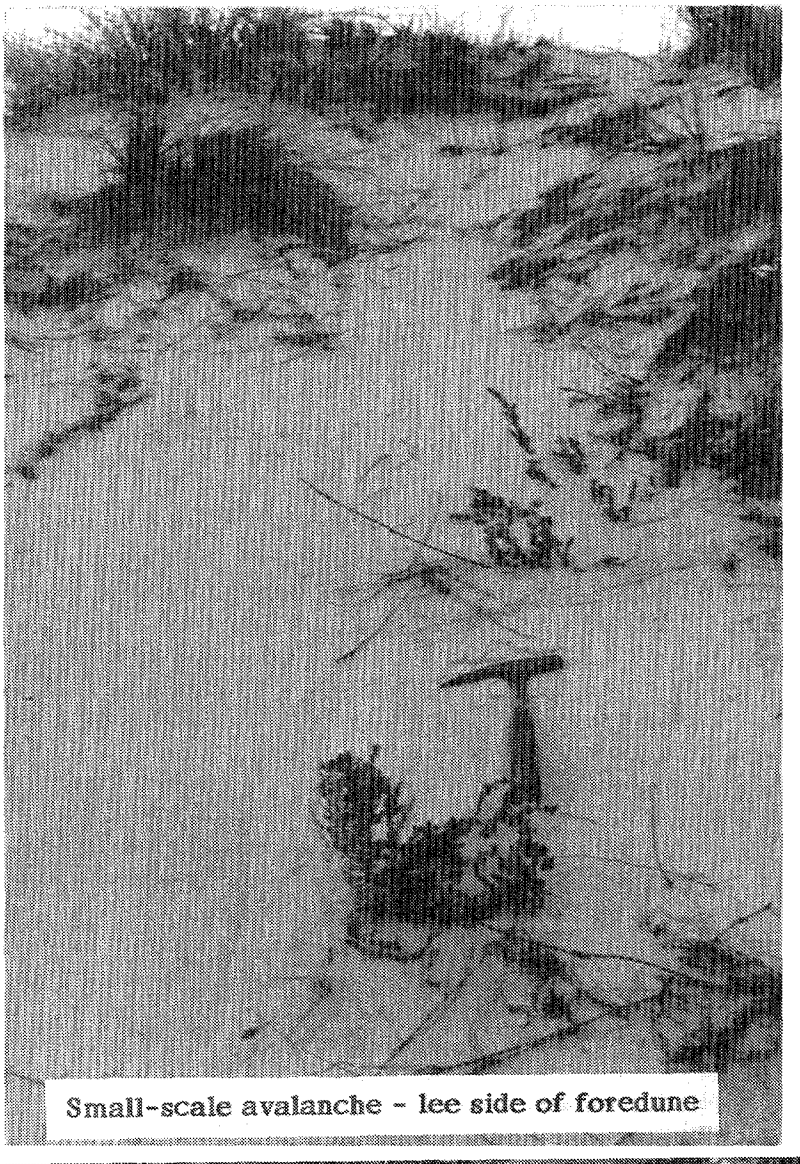

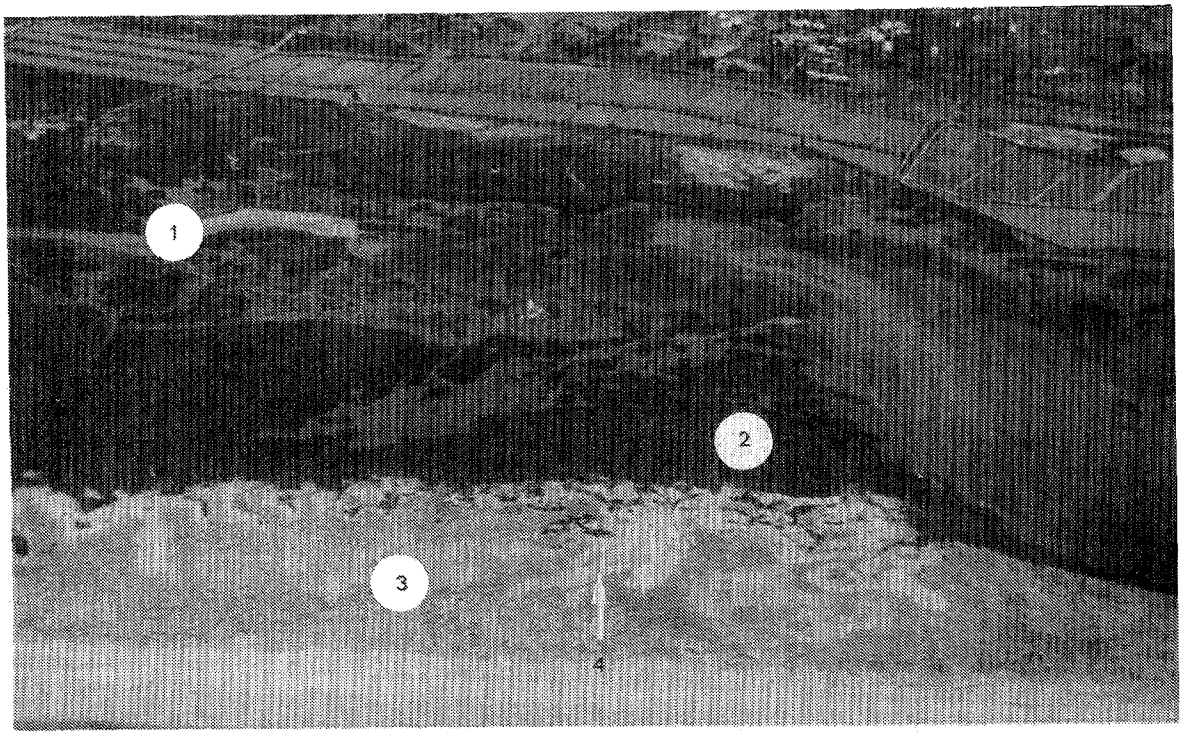

Fig. 8
Sand avalanche promoted by water-level carving (left) and oblique view of eastern Tavira island (below). **1** - main channel **2** - marsh **3** - backbarrier **4** - first-order channel.

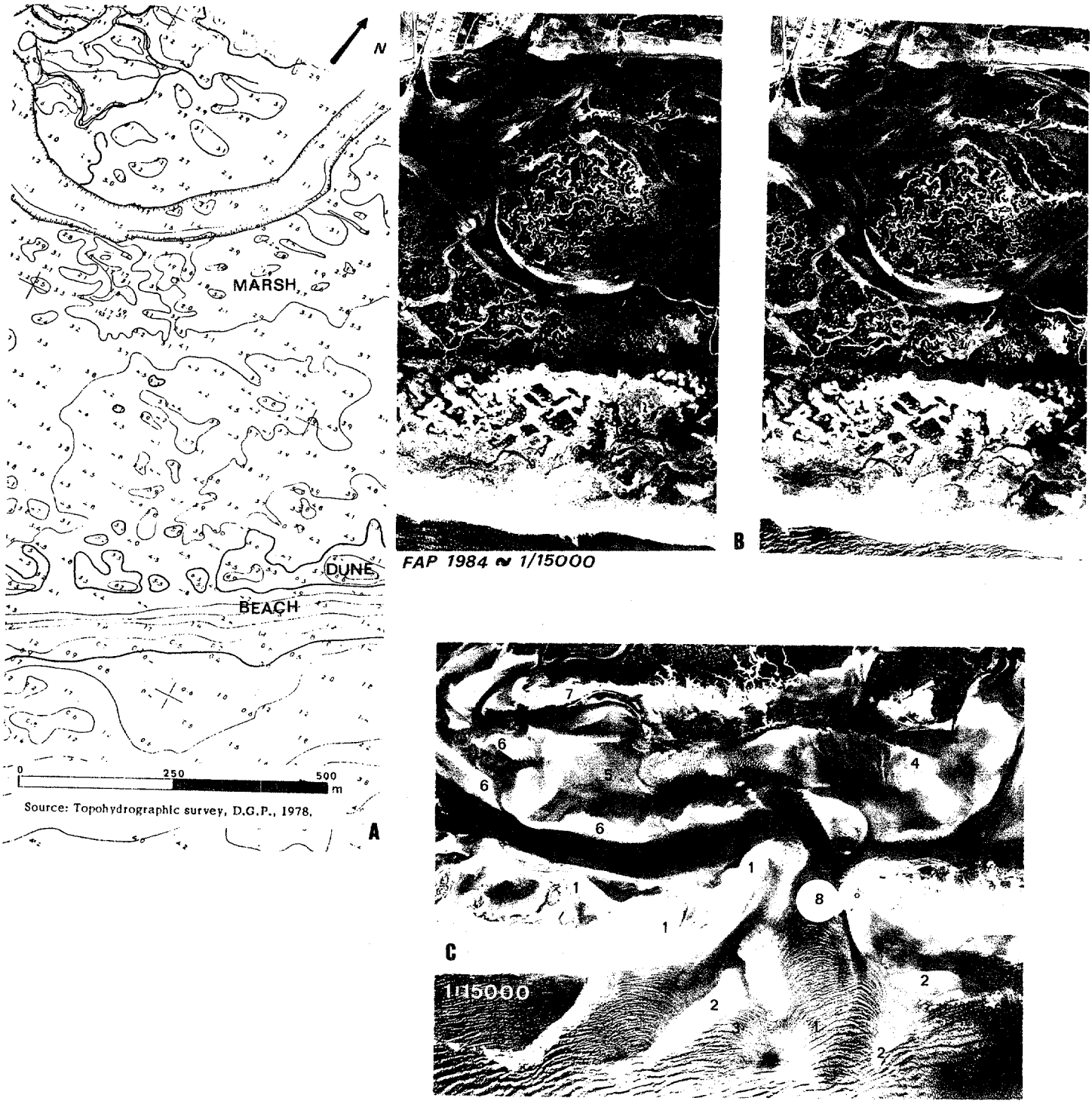

Fig. 9 - Topography (**A**) and stereoscopic image (**B**) of one relict tidal delta (squared area of fig. 5). Note "abandoned lobe" morphology on the left, chronical overwash of former channel gorge, first and second order channels.
Active inlet of Fuzeta (C). **1** - Recurved spits; **2** - Swash bars; **3** - Ebb delta (tide+swash ramp); **4** - Ebb shield; **5** - Abandoned lobe+spillovers; **6** - Reorganization of linear bars in an "echellon" chain; **7** - marsh island (abandoned, flood controled ebb shield, pressed against high marsh); **8** - Main channel gorge.

Similarity found between active and relict forms extends to the "abandoned lobe morphology", described by Andrade, 1990 at Ancão and Fuzeta inlets. This morphological pattern results from rapid translation of the inlet and starvation of the abandoned delta lobes generating an unusual discontinuous "en echellon" display of western ebb marginal spits cut off by short spillover lobes, reactivated by ebb currents.

It is postulated that these segments are relict flood-deltas, abandoned after a short period (10-20 years) of activity marked by rapid longshore drifting and mutual competition, ended by deactivation and closing by vertical agradation of a high berm, promoted by transverse sediment shifting, as depicted in Fig. 10.

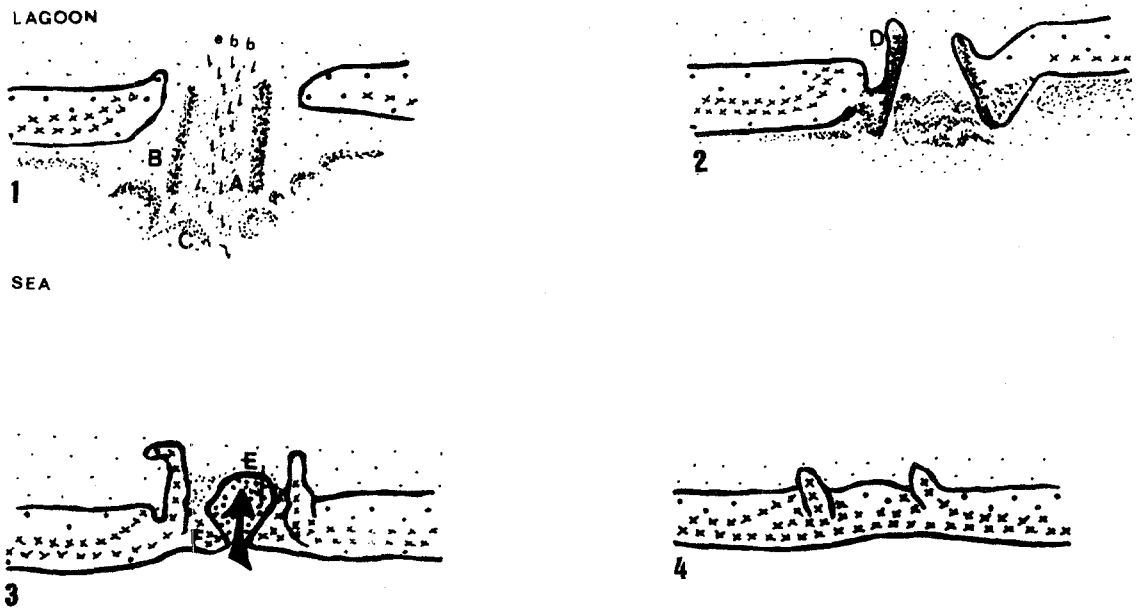

Fig. 10 - Interpreted deactivation sequence of a tidal inlet at Ria Formosa eastern barriers. 1 - An ebb channel is silting rapidly (**A**) favouring progradation of swash bars (**C**) over the ebb delta ramp (**B**). (2) Welding and landward displacement of swash bars plugg the channel. Linear bars are incorporated (**D**) and reshaped as recurved spits. An overwash intertidal surface is created, and agrades upwards. 3 - A beach berm develops (**E**), confined between transverse sand ridges. Upward accretion limits overwash ability and embryo foredunes take over, sealing the inner surface from further wave induced activity. 4 - A linear foredune develops and the external margin of the barrier heals completely.

4. The model

The following conceptual model is proposed to explain the morphological organization of the study area (Fig. 11):

A - Initial situation: A barrier (1) armoured with a low, discontinuous foredune ridge, strands into a developed intertidal marsh surface (2).

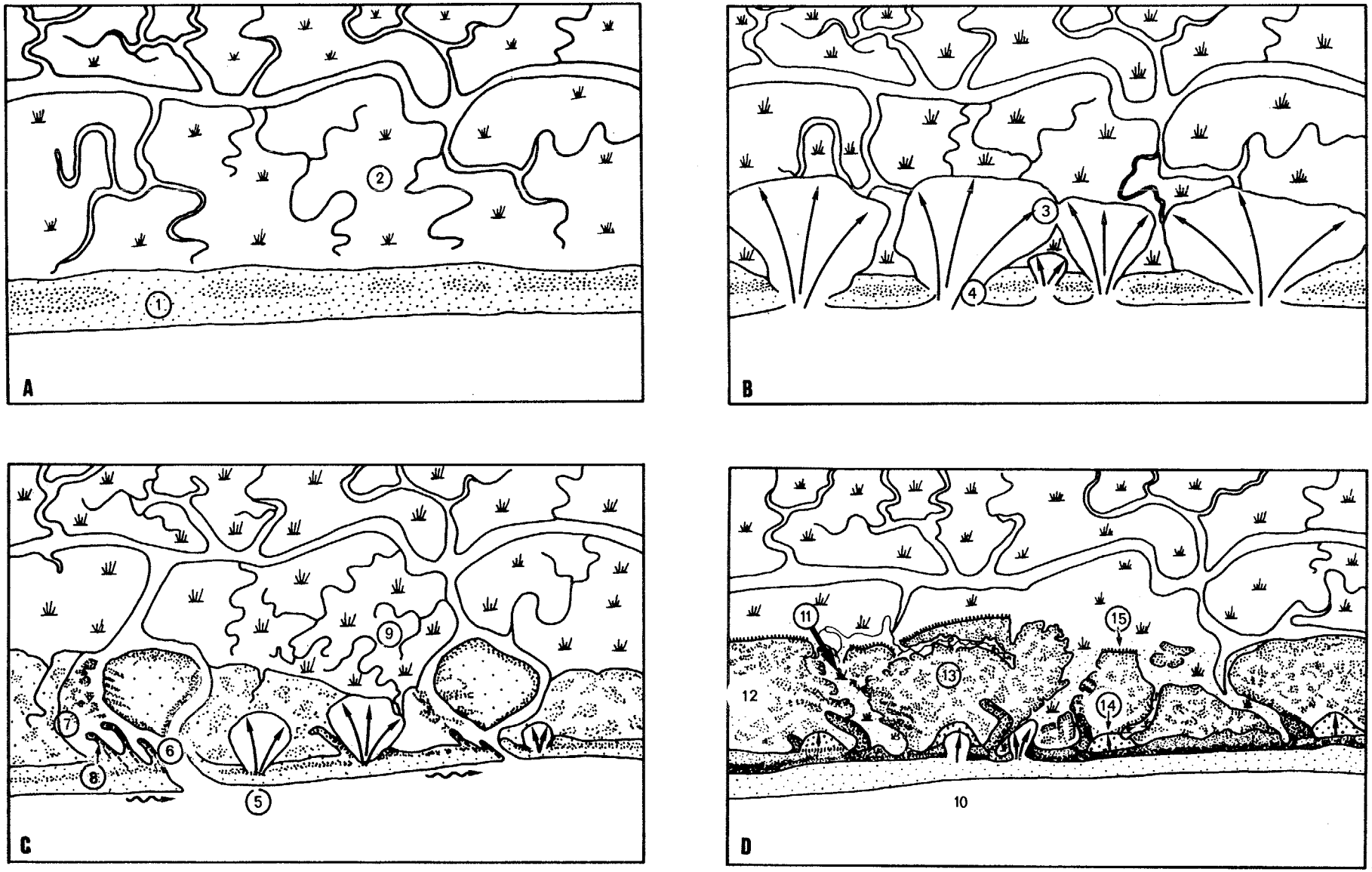

Fig. 11 - Proposed model for the morphologic framework of the study area. See text for explanation.

B - The 1755 tsunami hits the barrier, fully disrupting the former structure. A massive injection of sand covers the intertidal outer lagoonal surface, building an elevated platform (3) made of multiple coalescent washovers. A series of potencial tidal inlets is created (4) and backwater outlines the peripheral, future first order network.

C - Between 1755 and 1769 at least 4 other tsunamis repeat this cycle. Tidal prism accomodated by the lagoon is too small to cope with a large number of active, fast drifting inlets: unefficient structures close very quickly and become chronical overwash locations (5), while a small number of inlets develop typical tidal deltas (6). Rapid drifting generates abandoned lobe topography (7) of the western delta area and recurved tips develop at barrier tips (8). On the lagoonal side, smaller tributaries adapt to the newly imposed topography (9).

D - After 15 - 20 years the barrier is healed (10), and a second generation beach-foredune structure is added. Former peripheral channels adapt into the first order network (11) and convey tidal water through the sandy backbarrier platform (12). Lateral connection between nearby first order channels is ensoured in spring tide through a second order network (13), exploiting the low-lying surface of abandoned tidal delta lobes or ramps. Original morphology is etched and diluted by flood events and aeolian activity contributes to a thorough sand redistribution process. Terminal events of inlet deactivation and beach healing, immediatly followed by foredune establishment, are registered by relict overwash platforms (14), outcropping of the lee side of the foredune. The sand platform is reactiva ted and occasionaly scarped (15) both at the lagoonal and outer margins by tidal currents and small amplitude waves, generated by local wind blowing over the flooded surface in spring water.

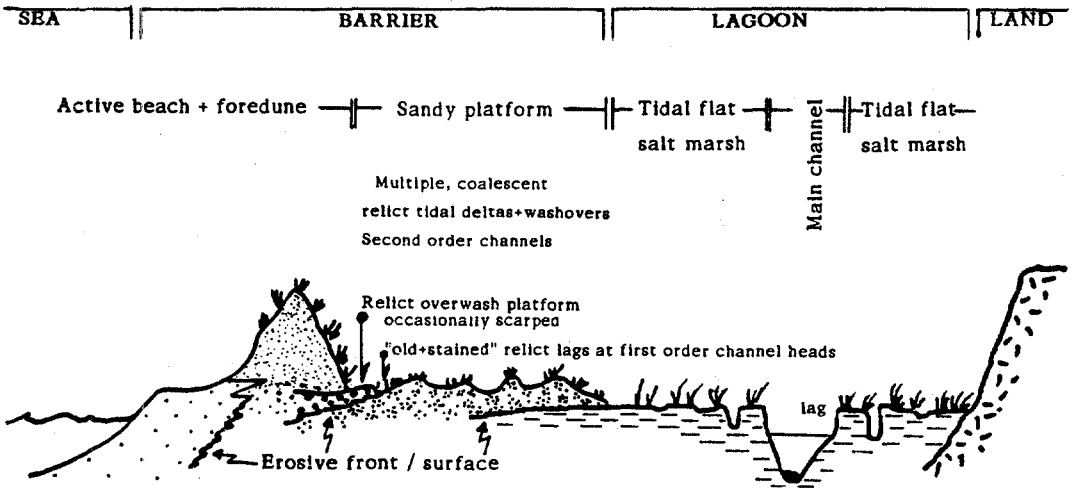

Fig. 12 - Proposed schematic cross section.

5. Conclusions

Dimensional and geometrical similarity found between different relict flood deltas strongly suggests that they are aproximately of the same age and that they have evolved during the same time lag.

An exceptionnaly largescale and intense overwash episode, different of a storm-generated event in the amount of energy input and overwash pattern, is required to account for the fea-

tures just described. A large tsunami would fulfill those requirements and provide the catastrophic change that ancient maps seem to describe in the period following the Lisbon Earthquake.

Further consequences of the proposed model are:

1. Tsunami activity may be the major forcing agent of large-scale barrier change and landward progradation of the barrier system of Ria Formosa, thus constituting a functional equivalent of hurricanes that generate seasonal retreat/rollover of other barrier chains (e.g. eastern United States).

2. Neotectonic activity (upwarping or rebound of the littoral-nearshore margin related with stress building along a major transverse accident) may be responsable for the elevation diference - approximately 0.4 m - found between relict and active tidal delta deposits.

Acknowledgements: This paper is a contribution and was partially supported by EEC-EPOC research contract CT-90-0015. The author thanks Dr. F. Marques for valuable discussions and help in the preparation of drawings and editing. Thanks are due to the Biblioteca Nacional (Dr. M.J.Feijão) and Dr. P. Bettencourt for facilities given in map research and reproduction.

References

Andrade, C. (1990) Estudo da susceptibilidade ao galgamento da Ria Formosa. Geolis, vol. IV (1, 2), pp 69-76.

Andrade, C. (1991) O ambiente de barreira da Ria Formosa (Algarve - Portugal). PhD Thesis, Dept. Geologia, Univ. Lisboa, 643 p.

Carter, R. (1988) Coastal environments. Academic Press, 617 p.

Hayes, M. (1979) Barrier island morphology as a function of tide and wave regime. In Leatherman (ed.) Barrier Islands. Academic Press, pp 1-29.

Hesp, P. (1988) Morphology, dynamics and internal stratification of some established foredunes in southeast Australia. Sed. Geol. (55), pp 17-41.

Mougenot, D. (1988) Géologie de la marge Portugaise. Thesis Doct. Etat, Univ. Paris, 257 p.

Pereira de Sousa, F. (1919-1932) O terremoto do 1° de Novembro de 1755 e um estudo demográfico.Vol. I-IV, I. Nacional, Lisboa.

Pessanha, L., Pires, H. (1981) Elementos sobre o clima de agitação marítima na costa sul do Algarve. Inst. Nac. Met. Geof., Lisboa, 67 p.

Pilkey, O., Neal, W., Monteiro, H., Dias, J.(1988) Algarve barrier islands: a non-coastal plain system in Portugal. Jour. Coast. Res., 5 (2), pp 239-261.

Pires. H., Pessanha, L. (1979) Agitação marítima na costa Portuguesa. Inst. Nac. Met. Geof., Lisboa, 13 p.

Ribeiro, A. et al. (1979) Introduction a la géologie générale du Portugal. Serv. Geol. Portugal, 114 p.

Romero, M.L. (1989) Epicentral parameters of Lisbon earthquake based on the study of the tsunami raised. Proc. Workshop on Historical Earthquakes in the Ibero-Maghrebian Region- Methodological Approach-Case Studies. Lab. Nac. Eng. Civil, Lisboa.

THE TSUNAMI SOCIETY

SCIENCE OF TSUNAMI HAZARDS

Publication Format for Camera-Ready Copy and Information for Authors:

1. Typing area shown by border.

2. One-column text.

3 All text must be typed single-space. Indent 5 spaces to start a new paragraph.

4. Page numbers in lower right hand corner in pencil or blue marker.

5. Top half of first page to contain the title in capitals, followed by the authors and author affiliation, centered on page.

6. Bottom half of first page to contain the abstract with the heading ABSTRACT centered on page.

7. Author must also enclose a separate sheet containing:
   - name and mailing address of senior author
   - one or two suggested index subjects
   - three to five keywords for cataloging
   - statement of any other submittal, publication, or presentation

8. Send original and a copy, with above information, to:

Dr. Tad Murty, Editor
Institute of Ocean Sciences
Box 6000
Sidney, B.C., V8L 4B2
CANADA

10" or 25 cm

7½" or 19 cm

TSUNAMIS IN THE MEDITERRANEAN AND PACIFIC AREAS: AN ANALYSIS

Di Maro R. and Maramai A.

Istituto Nazionale di Geofisica - Rome - Italy

Abstract

The aim of this study is to analyse some of the most important catalogues concerning Italian, Mediterranean and Pacific areas in order to obtain as much information as possible about tsunamis. Unfortunately, the data contained in the examined catalogues strictly depend on the different author's interpretations, because of the scarcity of the objective information: the instrumental data, that are only present in the Pacific catalogue.

With reference to this, we limited our data set only to data for which reliable observational information exist. For the other ones, we are going to make a deep revision of their historical sources in order to obtain, at least for the Italian area, a new analytical and more reliable catalogue. The results achieved from the data analysis will allow us to study the tsunami phenomena not only depending on the magnitude of the related event nor on the distance between the epicentral area and the coasts affected by tsunamis, but also on the coasts topography and on the water depth.

The study of tsunamis seems to be very interesting and, in the end, we propose a way to collect the existing data (parametral and digital ones) and to develop instrumental systems to better control and study this phenomenon.

Introduction

Tsunamis, like earthquakes and volcanic eruptions, are impressive natural phenomena that occur in many countries, often causing damages and fatalities. Fortunately, large tsunamis are quite rare, particularly in comparison with the great number of earthquakes of large magnitude which take place in all parts of the Earth. Nevertheless, tsunamis are a remarkable risk especially in a few areas of the world (Fig.1). This risk increases because of the uncertainties that still exist in understanding the behaviour of tsunamis. Our knowledge of tsunami evolution is incomplete,

because the generation phenomena have not been observed nor measured directly. In addition, such uncertainties are partly due to the poor attention that scientists gave to this phenomenon for many years. The interest of the scientific community has recently increased, also in areas (such as the Mediterranean Basin) in which tsunamis are not as large as in the Pacific, but neverthless noticeable.

Since ancient times tsunamis have been reported and documented extensively, especially in Japan and in the Mediterranean areas. The first ever recorded tsunami occurred off the coast of Syria in 2000 B.C. We know that most tsunamis occur in the Pacific Ocean, particularly in Japan, Peru, Chile, New Guinea and the Solomon Islands. However, the only regions that have generated remote-source tsunamis affecting the entire Pacific Basin are the Kamchatka Peninsula, the Aleutian Islands, the Gulf of Alaska and the coast of South America. Hawaii, because of its location in the center of the Pacific Basin, has experienced tsunamis generated in all parts of the Pacific. Even the Mediterranean Sea has some history of locally destructive tsunamis. Large tsunamis are very rare on the European and North African coasts. From literature on this subject we can see that there are two main tsunamigenic zones in the European area: the Eastern Mediterranean region, and the Gibraltar-Azores seismic line, situated southwest of Portugal. The region of the Straits of Messina (Southern Italy) is important too. Although in this area few tsunamis have been set off, usually they can reach high intensity (l.g. the tsunami associated with the 1908 Messina earthquake, Fig.2). Finally, only a few tsunamis have been generated in the Atlantic and Indian Oceans.

Data set

At present numerous catalogues on tsunamis are available in literature. They hold more or less complete historical and instrumental information about tsunamis occurring in the world, from which it is possible to start detailed analysis. Unfortunately, most of these catalogues, except for the Pacific one, are not analitical; therefore there are many difficulties and limitations to their use. In addition, as regards the Mediterranean area, quite a large number of catalogues written by several authors are available (Galanopoulos, 1960; Ambraseys, 1962; Moreira,1974; Antonopoulos, 1980; Soloviev, 1990; Caputo e Faita, 1984) but none of these collects data about the whole Mediterranean Basin.

In order to learn more about the real tsunami risk along the Mediterranean coasts, in 1988 a *World Laboratory* project, called "Assessment and Mitigation of Tsunami Hazard in the Mediterranea Area", was started, involving many countries as Greece, Italy, Portugal, Tunisia, Morocco, Spain, etc. In the frame of this project the Isti-

tuto Nazionale di Geofisica (ING) of Rome is preparing the first analitical catalogue for the Mediterranean area, particularly about the Italian tsunamis (Maramai and Gasparini, 1991). At present for the Italian coasts only the Caputo and Faita (1984) catalogue is available in literature, unfortunately not in analitical form. This catalogue reports Italian tsunamis from 79 B.C to 1954 A.D. and is the basis for the realization of the new analitical catalogue.

In this context, the aim of present work is to analyze some of the most important world-wide tsunamis catalogues already available in literature, both for the Mediterranean and Pacific areas, in order to know what kind of data they contain and what kind of studies they make possible.

The study was mainly based on the "National Oceanic and Atmospheric Administration" (NOAA, 1991) tsunamis data set, the Caputo and Faita Italian catalogue and the Soloviev Mediterranean catalogue. The NOAA data base is in two sections and collects data about many world-wide tsunamis, from 2000 B.C. to 1990, particularly those which occurred in the Pacific Ocean, but also regarding the Mediterranean Basin and the Atlantic Ocean. The first section is a file that holds information about 1953 tsunamigenic events and their main parameters (date, causes, geographic coordinates, magnitude, source area, etc.). Among those events, 74% referred to the Pacific Ocean, 16% referred to the Mediterranean and 10% concerned the Atlantic Ocean. The second file is much wider and more detailed; it contains the list of localities affected by each tsunami, with information on coordinates, travel-time of the wave, tsunami intensity, wave period, run-up, etc.

For the Mediterranean area, besides data contained in the NOAA data base, we used the catalogue published by Soloviev, that is the last one and more complete among catalogues regarding the Mediterranean Basin. This catalogue collects 300 tsunamis and sea level oscillations of unknown origin reported in the Mediterranean, from 1300 B.C. to 1981 A.C., and divides the Mediterranean into 18 zones in which tsunamis occurred (Fig.3a). In the Mediterranean basin the most tsunamigenic areas are along the coasts of Greece, particularly in the Aegean and Hellenic Arc; the Italian coasts are also quite prone to tsunamis, followed by Turkish, Jugoslavian and Albanian coasts.

As regards Italy, besides data reported in the above mentioned catalogues, we referred mainly to the catalogue already published by Caputo and Faita. It holds 154 events that occurred along the Italian coasts from 79 B.C. to 1954 A.D. and reports a list of the original bibliographical sources without any comment or interpretation. For this reason, this catalogue needs a careful revision in order to ascertain the real origin and the reliability of the listed phenomena. With reference to this, in Fig.3c we can observe, i.g., some tsunamigenic events located quite far from the coasts of Italy,

for which is difficult to believe the results. At present, we are carrying on a deep revision of Italian tsunamis which occurred along the coasts of Tuscany, Latium and Apulia, reported in the Caputo e Faita catalogue: from the first results it appears that some listed tsunamis are false or overstimated, particularly as regards minor events. This analysis has needeed quite a long time to be completed and definitive results will be published before long.

Data analysis

First of all, the analysis of the above mentioned catalogues pointed out that a lot of the examined data is not very reliable. In particular, we frequently have found events for which the lack of very important information like the date, geographic coordinates of origin, etc., is evident. Sometimes it is also possible to read in the catalogues about tsunamis as classified as being of seismic origin without the associated earthquake being present in any seismic catalogue.

In order to make a concrete analysis we excluded all questionable and erroneous events, to obtain a smaller but certainly more reliable data set. So, as regards the NOAA catalogue, we obtained a data set of 1241 events on which we could apply a statistical analysis.

First of all we classified the tsunamis on the basis of tsunamigenic causes. Fig.4 shows that approximately 90% of the tsunamis reported in the catalogues have a seismic origin. About 7% of the events are caused by volcanic eruption and only a few (2%) by landslides. We excluded all meteorological causes (1%) because of the unrelibility of the related tsunami.

Then we divided the data of the NOAA data set into three parts, on the basis of the origin area: Pacific Ocean, Atlantic Ocean and Mediterranean Basin. Analysing Figs.5-7 we can see, as expected, the prevalence of the Pacific data in comparison with the other two zones, especially regarding the last century. The large amount of data for this period is also certanly due to the remarkable development of the instrumentation (tide-gauges) along the Pacific coasts. With reference to this, in Fig.8 the percentage of the events versus the maximum run-up values, is shown. A clear predominance of events with a moderate run-up elevation is noticeble, mostly below 1 meter, all recorded in the Pacific area. On the contrary, the Italian and Mediterranean catalogues report only observational information, without any kind of instrumental recording. Unfortunately during the last century in the Mediterranean Basin the decreasing of the observational practice has not been adequately supported by an instrumental development.

As regards the Mediterranean Basin, we compared data contained in the three

examined catalogues (Caputo and Faita, 1984; Soloviev, 1990; NOAA, 1991), bearing in mind that Caputo's catalogue refers only to the Italian area. From the three catalogues we excluded all doubtful and erroneous events as well as tsunamis for which the epicentral coordinates are not reported. Therefore, we obtained a data set of 87 events for the Caputo's catalogue, 55 tsunamis for the Soloviev's catalogue and 102 events for the NOAA.

Making a comparison (Figs.3a-c), first of all it can be pointed out that there is an evident difference in the quantity of the information available in the three catalogues, especially as regards Italian tsunamis. In fact, we can note (Fig.3c) that the NOAA catalogue collects only one event which occurred along Italian coasts, the one that followed the Messina, December 1908 earthquake. Really, this is the strongest Italian tsunami and the only one remarkable enough to kindle the interest of the international scientific community, but nevertheless the occurrence of some other relevant tsunami has been verified. The catalogue of Soloviev draws inspiration from the data contained in the Caputo catalogue as regards the Italian area, while for the Mediterranean Basin it is in good accordance with the NOAA data set. It should be emphasized that the discrepancy in the quantity of information present in the three data sets does not arise from apparently known causes, except for the interpretation of phenomena. In fact, some authors ascribed as tsunami some visible effects (i.g. the presence of some shells in a field quite away from the coast) that other authors did not interpretate as a tsunami.

Finally, we focused our attention on the run-up elevation in order to analyse its correlation with some other parameters of the tsunamigenic earthquake; we can observe that it is possible to have two or more different run-up values corresponding at the same magnitude value. Figures 9-10 show that an increase in magnitude value does not produce a clear increase in run-up. Similar behaviour has been pointed out analysing the run-up trend versus epicentral distance for different magnitude values. From Fig.11 (three-dimensional graph) we can observe the behaviour of the above mentioned variables: run-up, magnitude and epicentral distance. On the whole, we cannot identify a well defined trend, except for the strongest events occurred very close to the tsunami source: for this kind of events the maximum run-up values is observed. As the rest, the unreliability of the data does not allow us further interpretations.

During this research, we also have tried to analyse the focal mechanisms of some tsunamigenic earthquakes, in order to find a relation between them and the behavour of the sea. This study was possible only for very few events because of the insufficiency of reliable data about both focal mechanisms and tsunami information. In particular, we tried to relate the first motion of the ground (compressions and dilata-

tions) to the first movement of the wave (rise or fall) but, also for the well documented events, we could not find any certain connection.

At present, because of data uncertainty, we are not yet able to distinguish the roles played by some decisive factors, for example, bottom sea topography, coastline, earthquake magnitude value, epicentral distance, etc. and, consequentely, the importance of such factors in the determination of the tsunami itself.

Conclusions

From the results of this study we can infer that data reported in the examined catalogues are extremely difficult to process: apart from the usual problems arising from the use of catalogues (completeness and reliability of data set), we find that most of the information are not in digital form. In addition, the catalogues available present different quality and quantity of data that makes the unification of all information in a single catalogue very hard.

In particular, the examination of the three catalogues shows that, at present, the available data do not allow us to obtain reliable results from the statistical analysis, principally because of the necessity to only use really concrete data, so obtaining numerically reduced data sets.

We suggest, at least for the Mediterranean area, a critical revision of data reported in the catalogues, in order to obtain a single, complete and realiable catalogue with a sufficient grade of coherence. For the future, expecially for the coasts of the Mediterranean regions, it appears also necessary to improve the use of tide-gauges with the aim to obtain a network recording data directly in digital form, to constitute a basis for more significant elaboration. From this point of view is as important to install more instruments as to collect and digitized the the already acquired analogical data, that constitute an important scientific patrimony to save and that, unfortunately, are often lost or in bad repair.

References

Ambraseys N.N., 1962; *Data for the investigation of the seismic sea waves in the Eastern Mediterranean*; Bull.Seism.Soc.Am., 52, 4, 895-913, Berkeley.

Antonopoulos J., 1980; *Data from investigation of seismic sea-wave events in the Eastern Mediterranean from the birth of Christ to 1980 AD*; Annali del Geofizica, 33, 141-248.

Caputo M. and Faita G., 1984; *Primo catalogo dei maremoti delle coste italiane*; Atti Accademia Naz. Lincei- Classe di Sc.Fisiche,Matem. e Nat.- Serie VIII, Vol. XVII - Anno CCCLXXXI, Rome.

Galanopoulos A.G., 1960; *Tsunamis observed on the coasts of Greece from antiquity to present time*; Ann.Geof., XIII, 3-4, Rome.

Maramai A. and Gasparini C., 1991; *A proposal for a new catalog on tsunamis in the Mediterranean area*; Science of Tsunami Haz., vol.9, n.1, 39-46.

Moreira S.V., 1974; *Earthquakes and tsunamis in the European area*; Proceed. XIIIth General Assembly of the European Seismological Commission, Bucharest.

NOAA - National Oceanic and Atmospheric Administration, 1991; *World-Wide Tsunamis 2000 B.C.-1990*; World Data Center A for Solid Earth Geophysics, U.S. Department of Commerce - National Geophysical Data Center, Boulder, Colorado -U.S.A.

Soloviev S.L., 1990; *Tsunamigenic Zones in the Mediterranean Sea*; Natural Hazard, 3, 183-202.

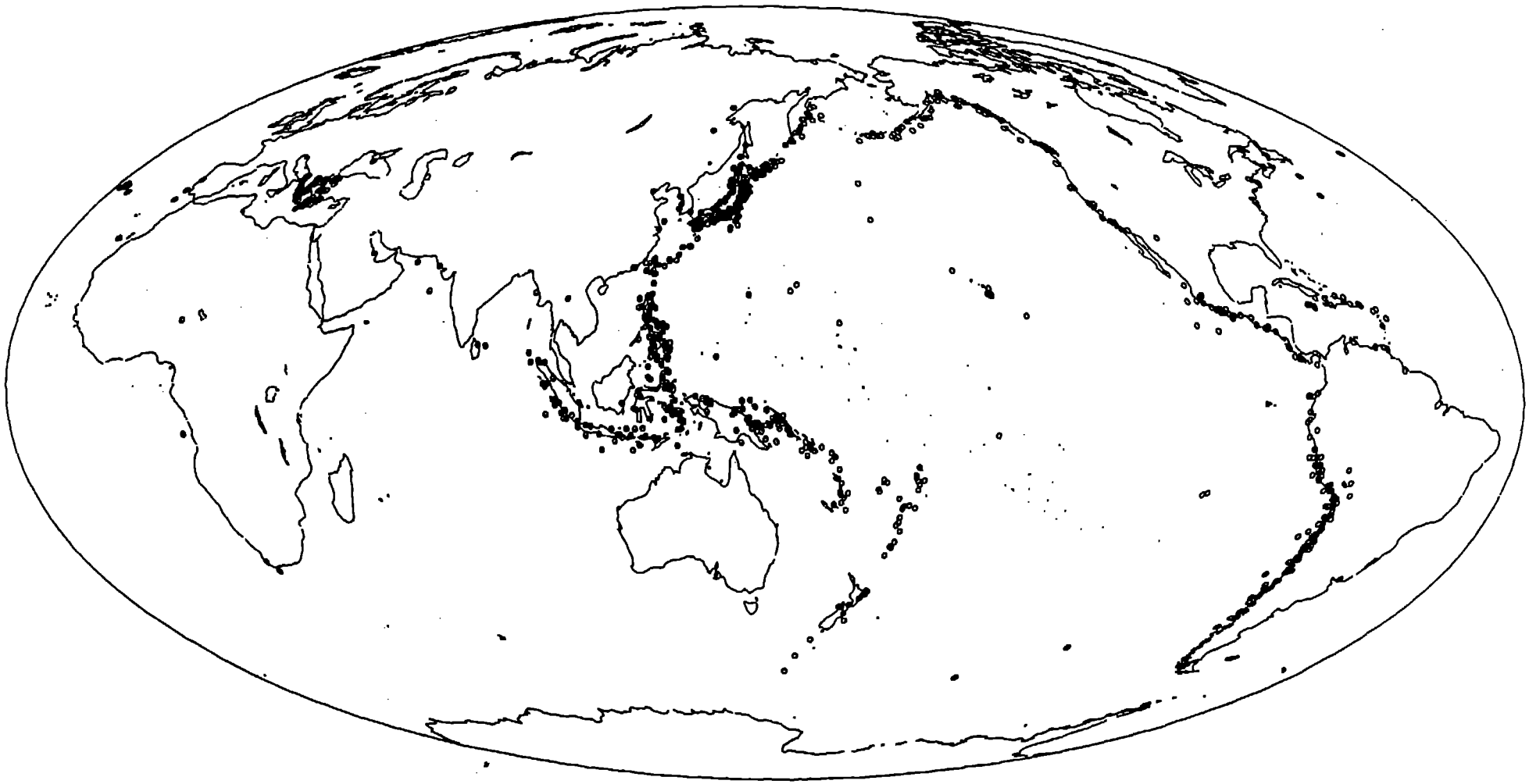

MOLLWEIDE EQUIVALENT PROJECTION

LATITUDE CENTER = 0.0

LONGITUDE CENTER = 150.0

Fig.1 - World-wide distribution of tsunamigenic events (2000 B.C.-1990 A.C.)

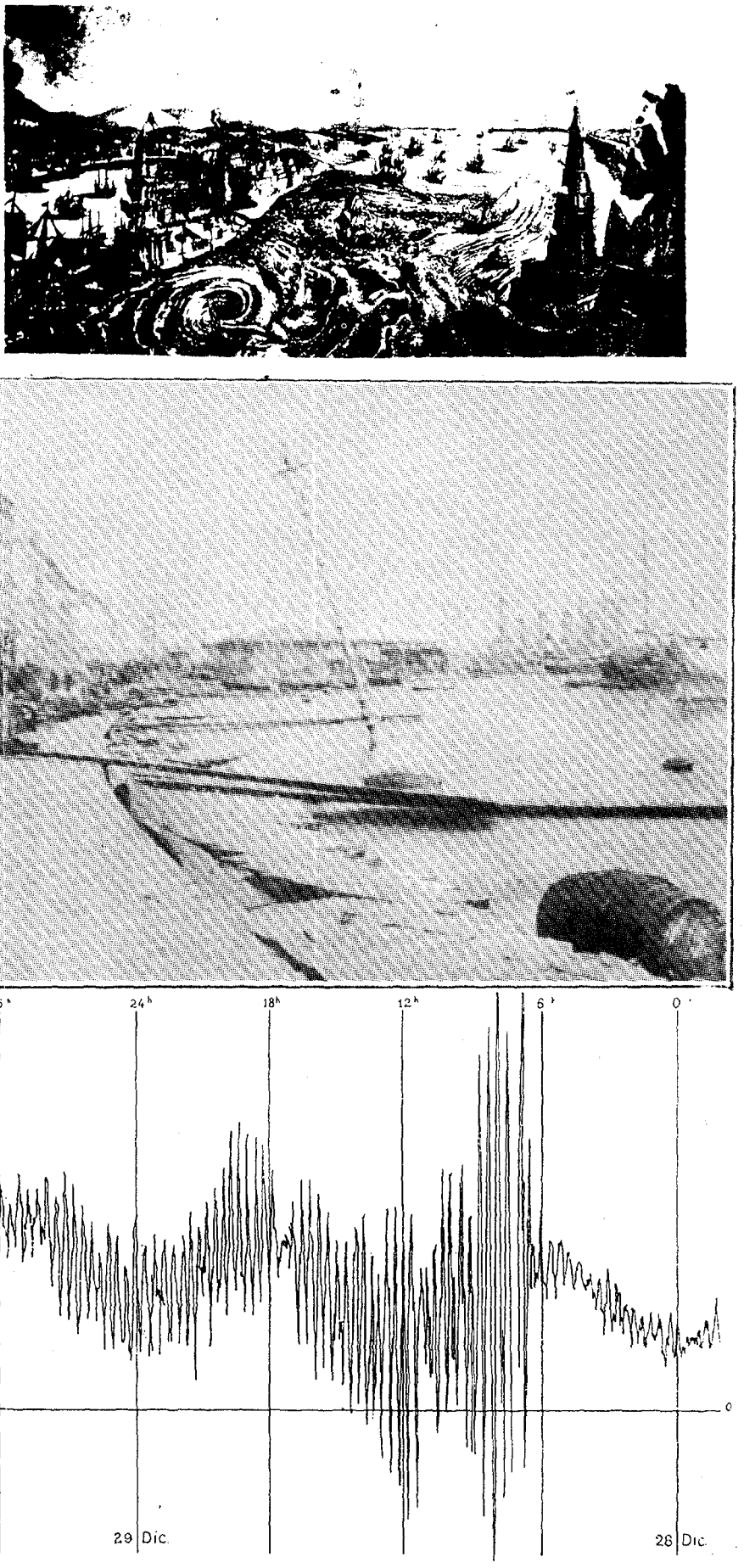

Fig.2 - Three different "points of wiew" for a tsunami (Messina, 1908): a) an imaginative view taken from an artistic painting; b) real severe damages at Messina harbour; c tide-gauge record.

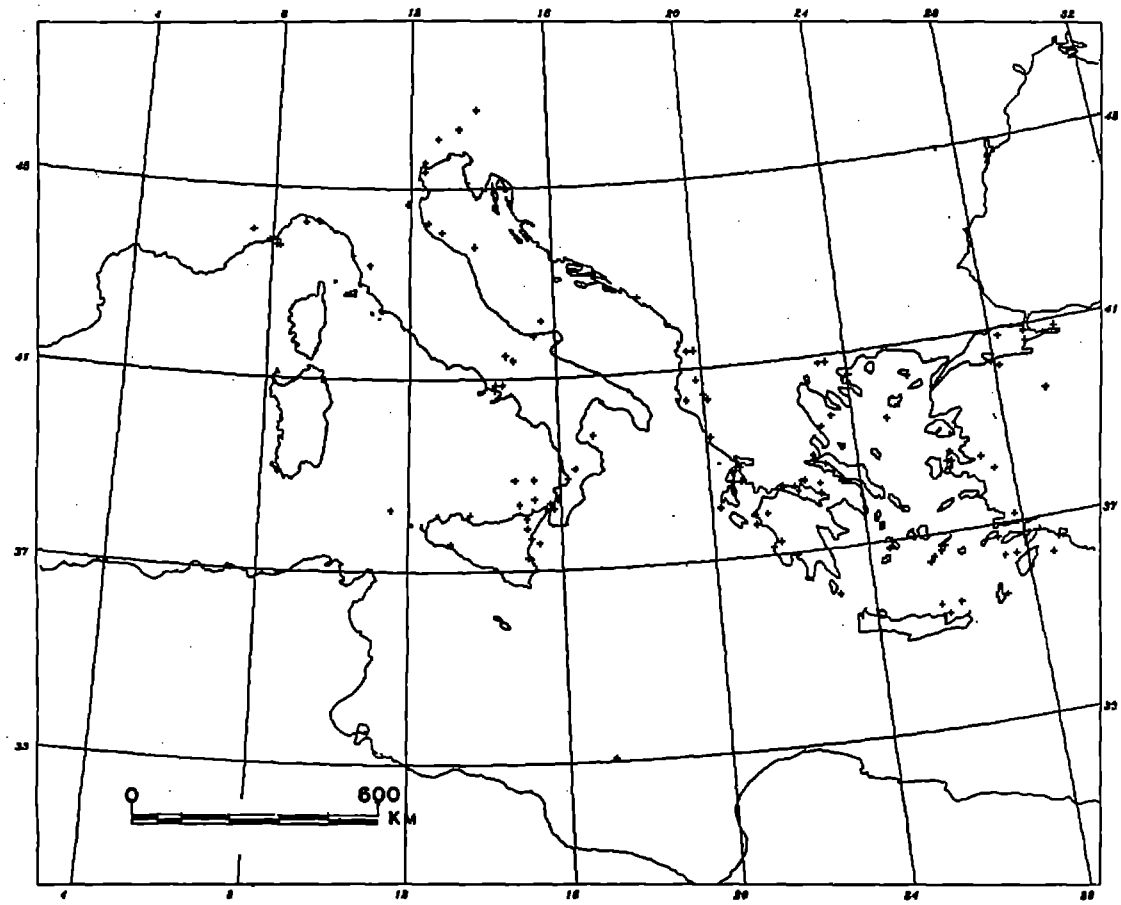

Figure 3A

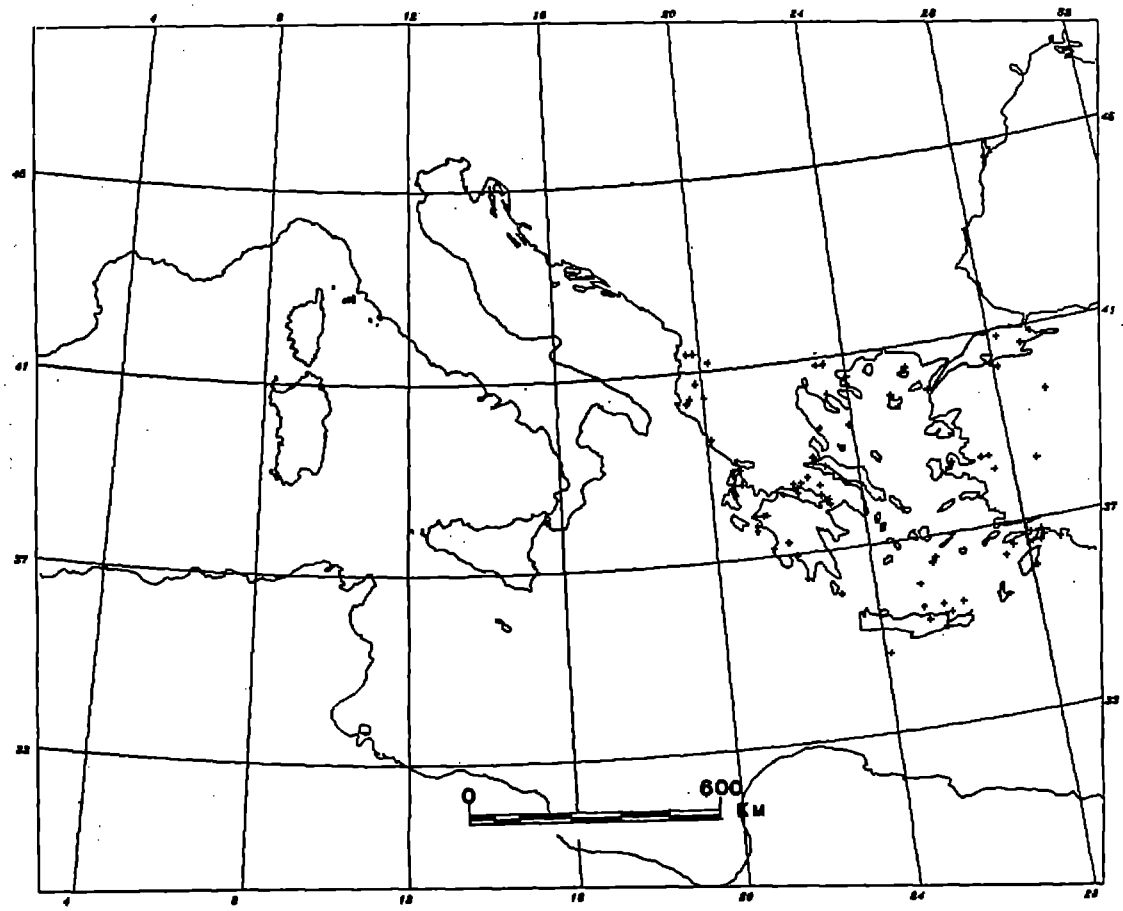

Figure 3B

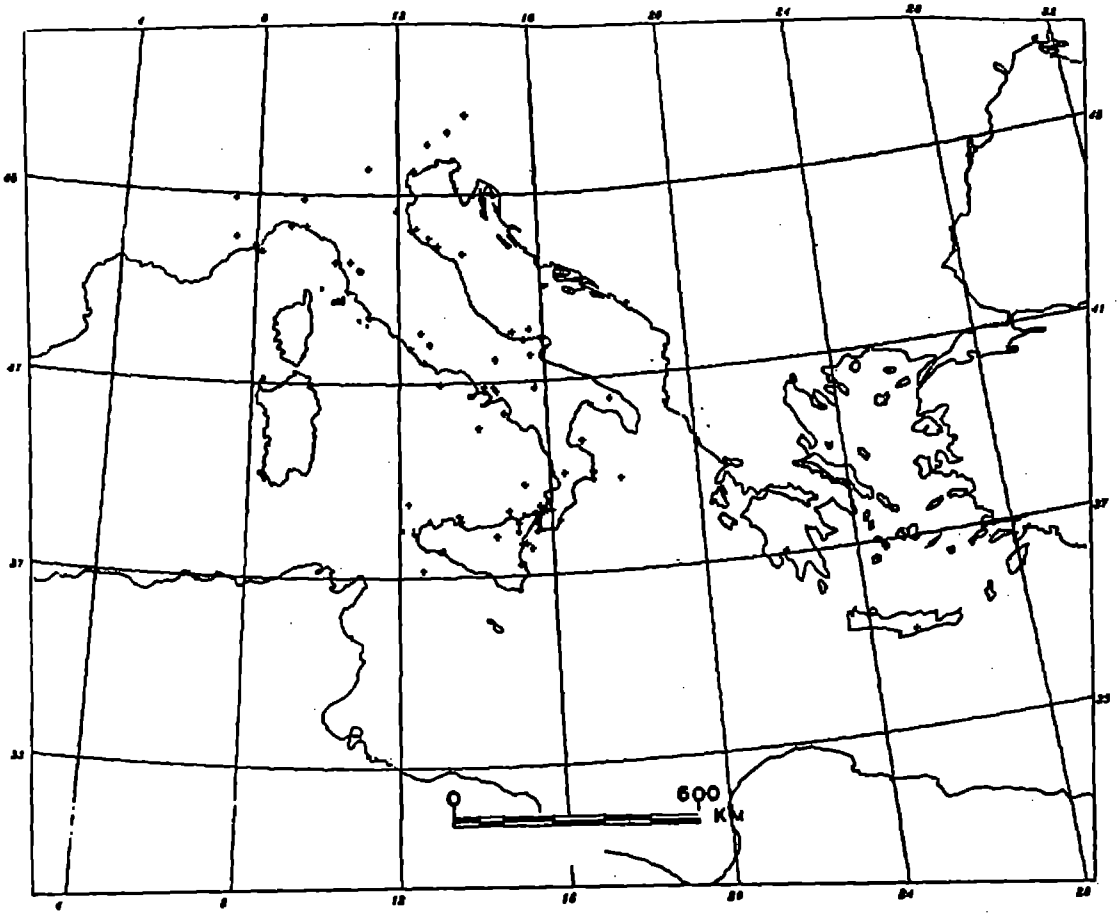

Figure 3C

Fig.3 - Tsunamigenic events in the Mediterranean Basin (2000 B.C.-1990 A.C.) **a)** data collected by Soloviev (1380 B.C.-1979 A.C.); **b)** data collected by NOAA (2000 B.C.-1990 A.C.); **c)** data collected by Caputo and Faita for the Italian coasts only (79 A.C.-1979 A.C.).

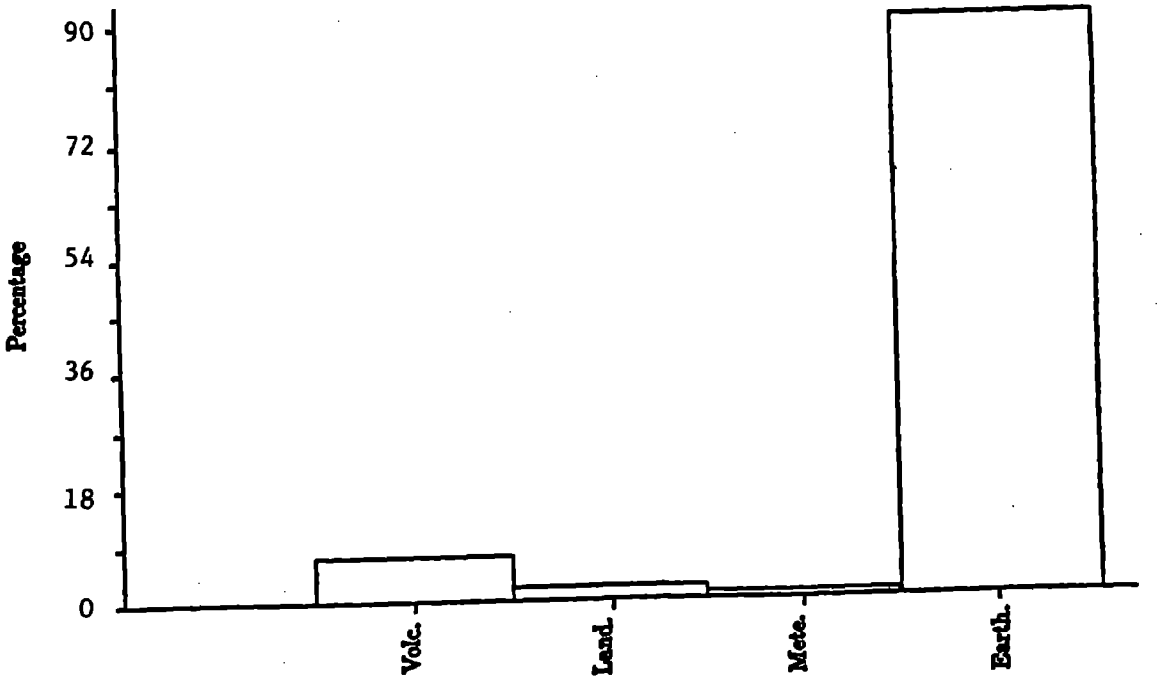

Fig.4 - Percentage of the main causes of tsunamigenic events.

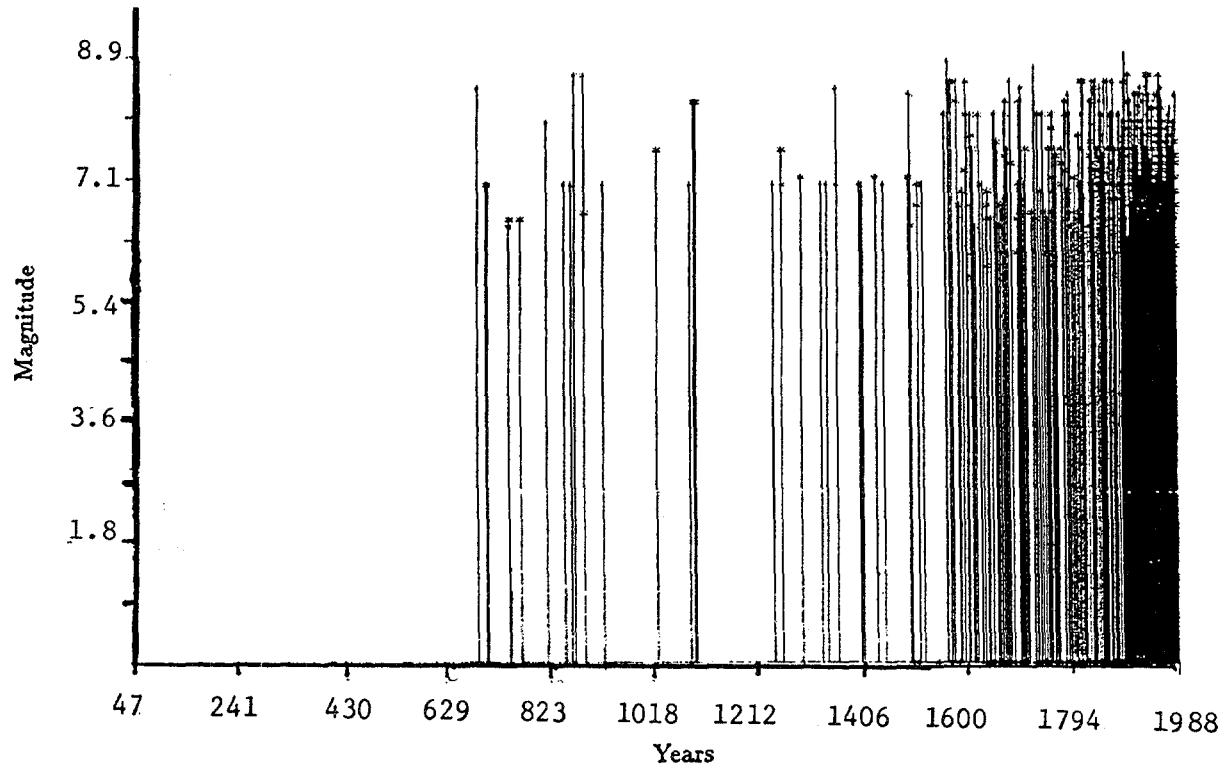

Fig.5 - Temporal distribution of tsunamis for the Pacific area.

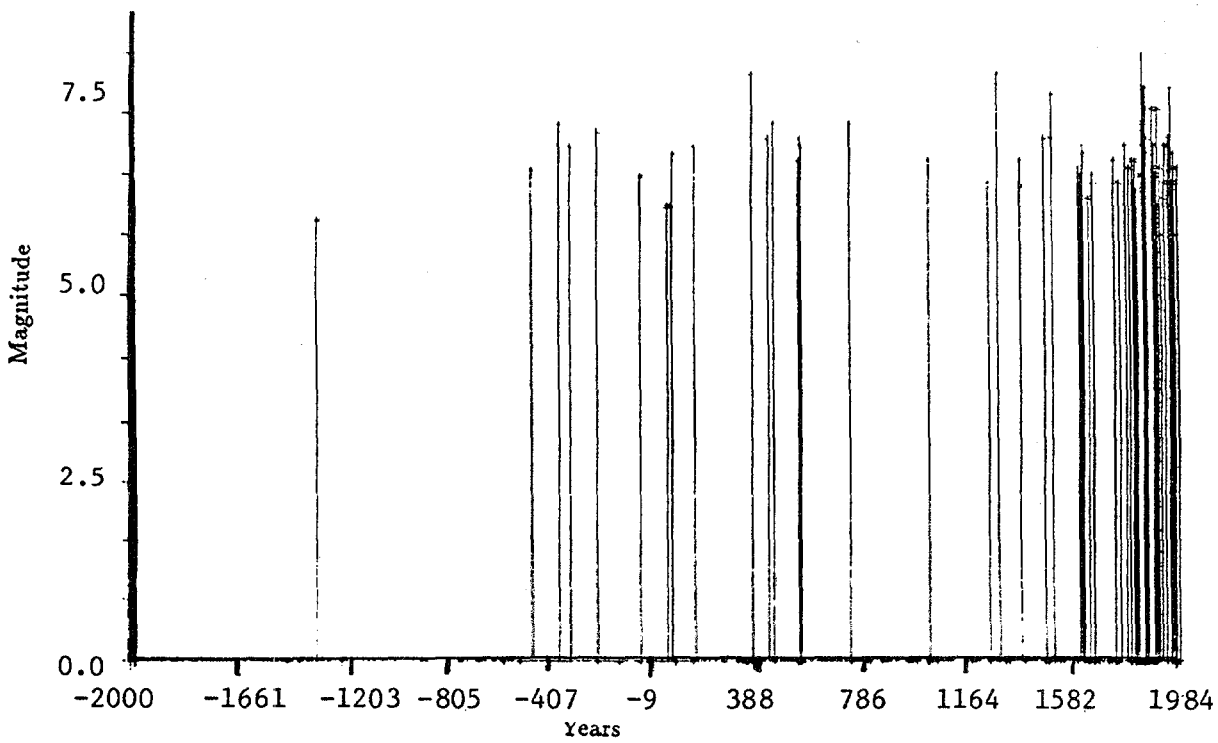

Fig.6 - Temporal distribution of tsunamis for the Atlantic area.

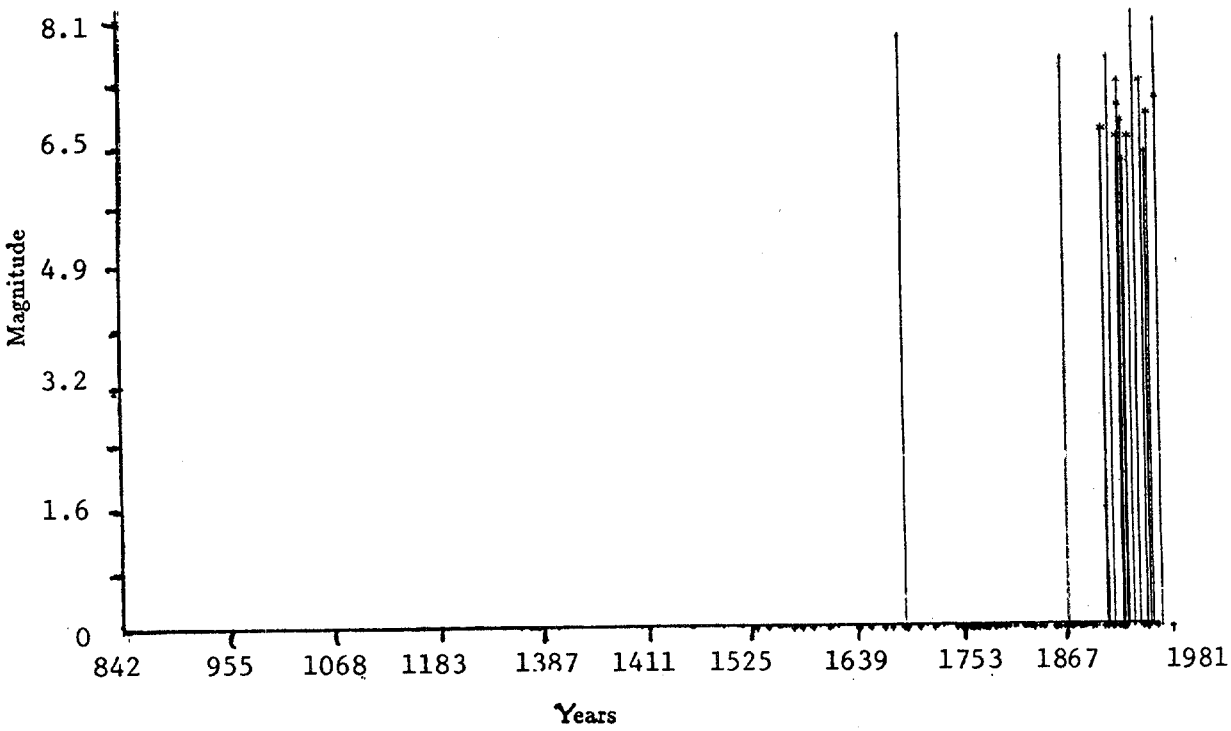

Fig.7 - Temporal distribution of tsunamis for the Mediterranean Basin.

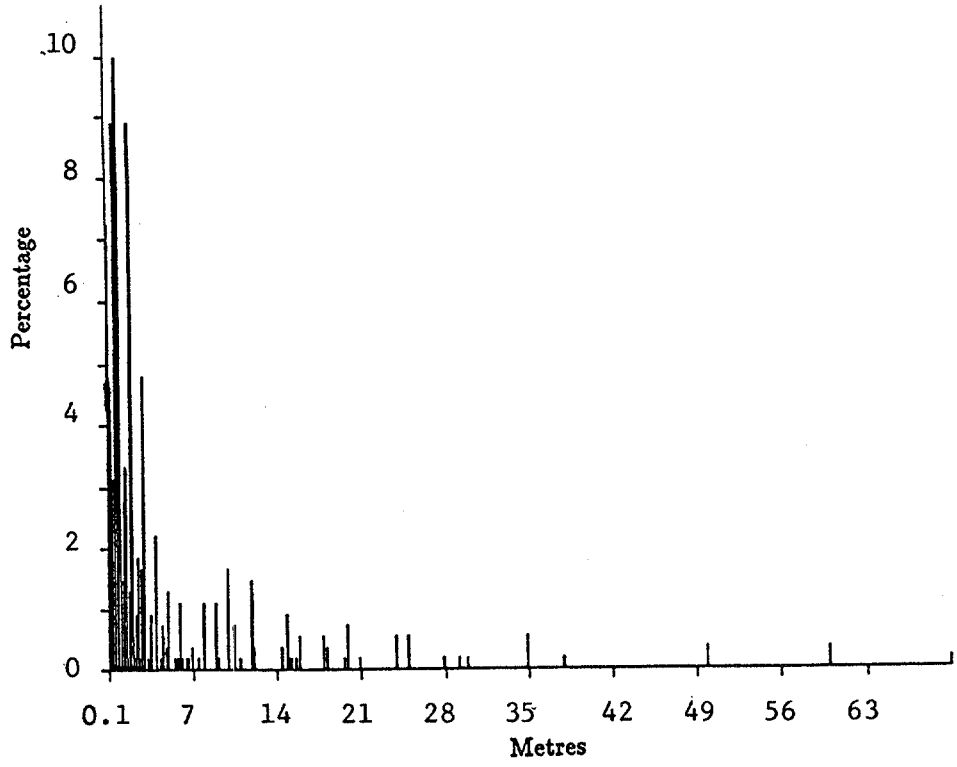

Fig.8 - Percentage of events versus maximum run-up values (from the NOAA data set) for all the three areas.

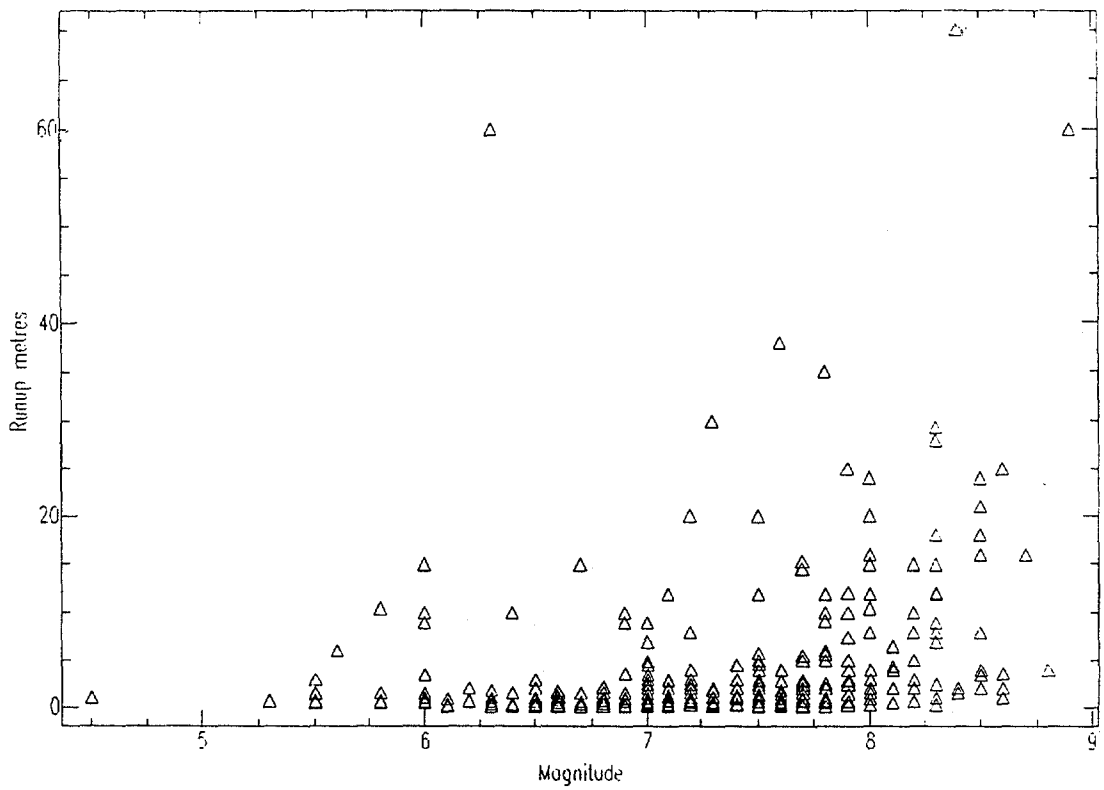

Fig.9 - Tsunami run-up versus magnitude of the related event for the Pacific.

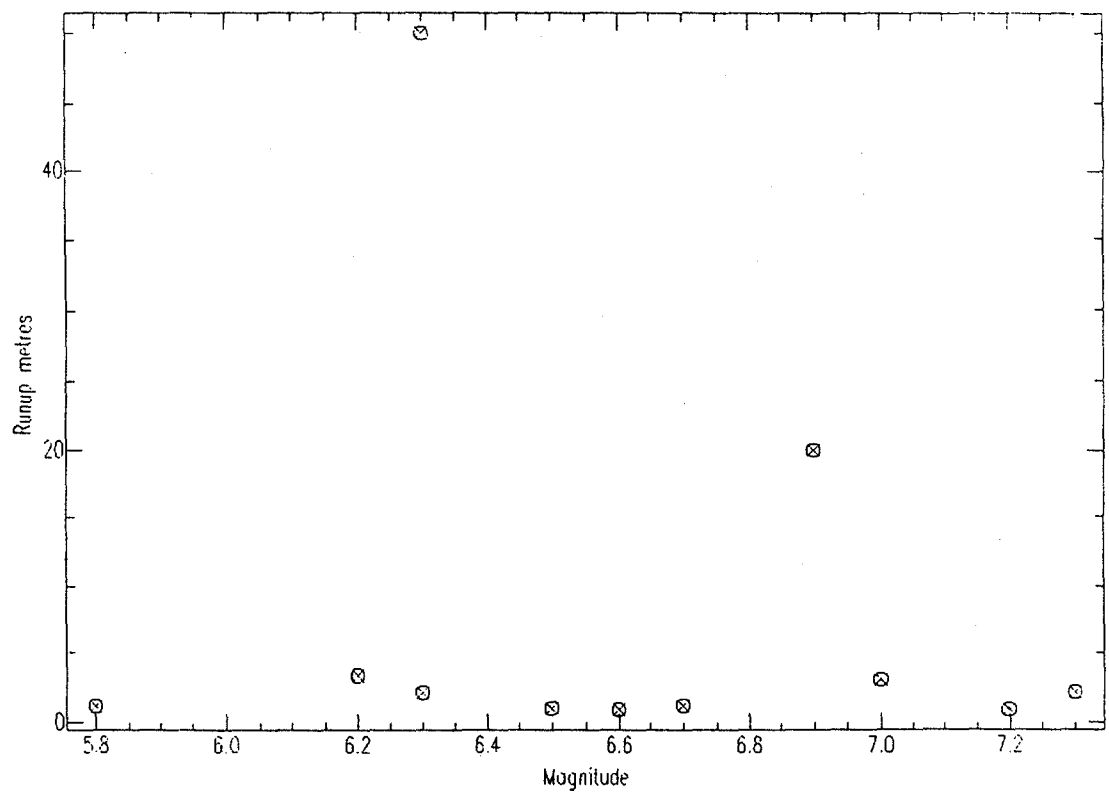

Fig.10 - Tsunami run-up versus magnitude of the related event for the Mediterranean area.

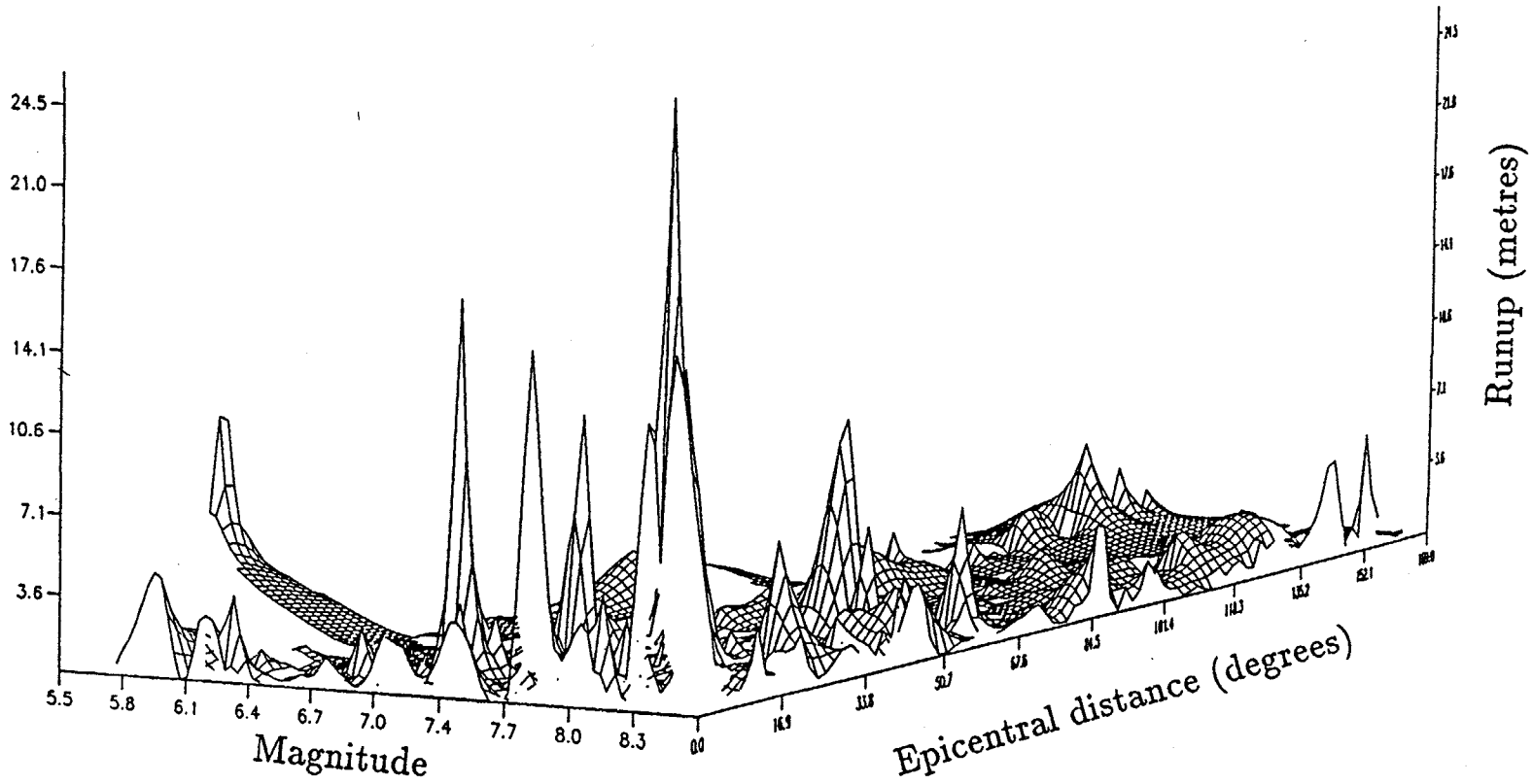

Fig.11 - Maximum run-up value versus magnitude versus epicentral distance obtained from the NOAA data set, from 1900 A.C. to 1990 A.C.

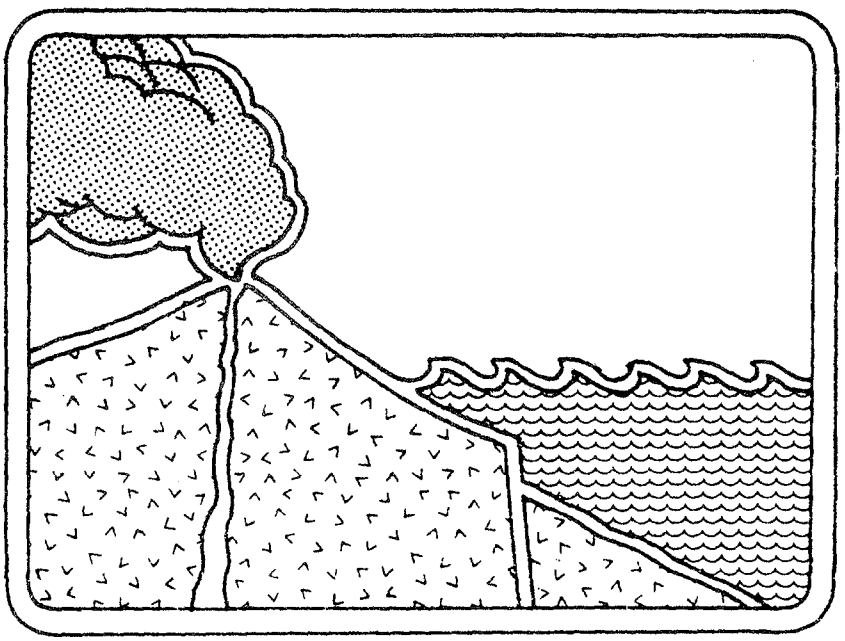

MODEL STUDIES OF THE EFFECTS OF THE STOREGGA SLIDE TSUNAMI

R.F. HENRY AND T.S. MURTY

Institute of Ocean Sciences
Department of Fisheries and Oceans
P.O. Box 6000, Sidney, B.C. V8L 4B2, Canada

ABSTRACT

Recent evidence from sand deposits on the east coast of Scotland support the idea that a major submarine slide off the coast of Norway between 8000 and 5000 years B.P. (the second Storegga slide) caused a tsunami in the North Sea (Dawson et al., 1988). A distinctive sand layer dated to this period has been observed in beach sediments from the Dornoch Firth to just south of Dunbar. Although this deposit could conceivably have been caused by a storm surge, the high water velocities needed to scour sufficient bottom material would more likely to have occurred during a tsunami. A numerical model could help to resolve this question, as well as indicating possible other coastal locations where the tsunami amplitudes were great enough to have caused similar deposits.

Based on data available on the dimensions of the slide (Jansen et al., 1987) an analytical model gives a value of about 12m for the tsunami amplitude at the source. The same one-dimensional model gives a rough estimate of about 4m amplitude at the Scottish coast, but realistic topography is not adequately represented in the analytical model. A two-dimensional finite-difference model was used to simulate the propagation of the tsunami from the Storegga site and estimate the resulting amplitudes along the opposite coasts.

1. INTRODUCTION

Dawson et al. (1988) and Long et al. (1989) discussed the evidence on the east coast of Scotland for a possible tsunami that could have occurred following the so-called Storegga submarine landslide off the coast of Norway. Harbitz (1992) numerically simulated the tsunami generated by this slide, taking into account the detailed mechanism of the slide and its effects on the generated tsunami. He shows contours of the tsunami amplitude on the coasts of Norway, Greenland, Iceland and north coast of Scotland. He does not show any results for the east coast of Scotland.

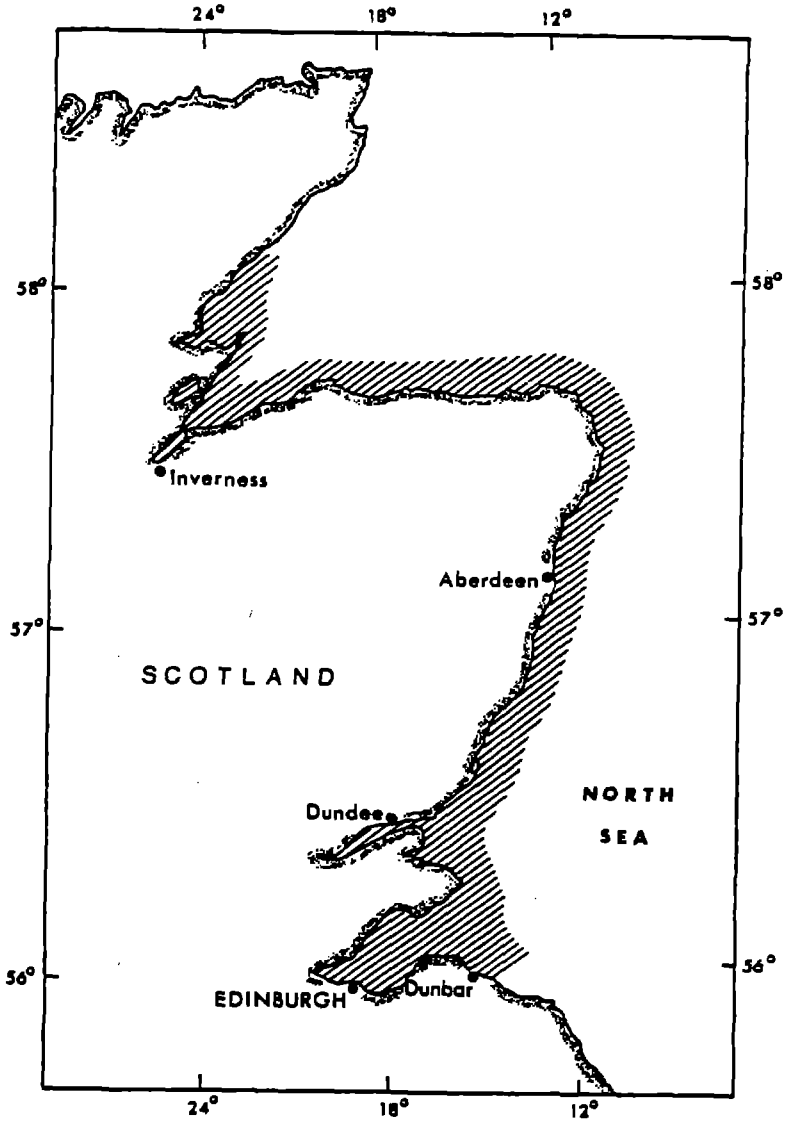

Figure 1 *Extent of coastline (shown hatched) including sites with sand sediments possibly attributable to the second Storegga slide tsunami.*

Our study differs from that of Harbitz at least in two respects. We did not simulate the slide itself. Using the volume of the slide that is quoted in the literature, we estimated through simple analytical formulae that the initial amplitude of the tsunami at the source could have been about 10m, but probably not less than 8m and not more than 12m. We then propagated the tsunami to the east coast of Scotland, rather than the north coast, using a fairly standard two-dimensional numerical model. Even though we show results for the North Sea, our emphasis is mainly on the east coast of Scotland, especially for the hatched area shown in Figure 1, where tsunami deposits of sand layers have been observed.

2. A SIMPLE ANALYTICAL MODEL

Various empirical relations are available in the literature for computing the tsunami amplitude at the source due to a submarine landslide (e.g., Striem and Miloh, 1975; Raney and Butler, 1975; Slingerland and Voight, 1982; Murty, 1979 and Wigen et al., 1983). The relationship has the following general form

$$\ln\left[\frac{\eta}{D}\right] = K_1 + K_2 \ln\left[\frac{V}{D^3}\right] \qquad (1)$$

where η is the maximum tsunami amplitude at the source, D is the average water depth at the source and V is the volume of displaced material during the submarine slide. Here both η and D are expressed in km and V is in km^3. Different authors give different values for the coefficients K_1 and K_2.

The water depth in the source area for the second Storegga slide tsunami is in the 500m to 1 km range and the volume of the slide material is estimated to be between 700 and 1700 km^3. Thus in a very approximate manner we estimated that the maximum tsunami amplitude at the source could have been as high as 12m, but was probably somewhat less.

Again in the literature there are several empirical studies dealing with dispersion of tsunami waves (e.g. Murty, 1977; Wang et al., 1987). Based on observations of

tsunami travel over long distances (greater than a few hundred kilometers) over relatively deep water and in the absence of too many topographic irregularities and islands, it was deduced that the tsunami amplitudes y_2 and y_1 and distances x_2 and x_1 from the source could have the following relationship

$$y_2 - y_1 = c(x_2 - x_1) \tag{2}$$

The coefficient has different values for different ranges. In the 500 to 1000 km range, $c = -1 \times 10^{-5}$ approximately (when x_1, x_2, y_1, y_2 are expressed in m).

Taking $x_1 = 0$ (source) and $y_1 = 12$m and for $x_2 \sim 800$ km (approximate distance of the source to the coast of Scotland)

$$y_2 - 12 = -1 \times 10^{-5} (8 \times 10^5 - 0)$$

or

$$y_2 = 12 - 8 = 4\text{m}.$$

which in a very rough sense is about the maximum observed tsunami amplitude on the coast of Scotland.

3. A TWO-DIMENSIONAL NUMERICAL MODEL

Even though for large travel distances, a spherical polar coordinate system is preferable, for simplicity and convenience we used a right-handed Cartesian coordinate system. The water depths in the computational domain are shown in Figure 2. The square grid for the numerical computation is shown in Figure 3 and the size of each grid element is 18.55 km. The partly linearized shallow water equations are (the subscripts denote differentition) (Henry, 1982; Murty, 1977, 1984):

$$\eta_t = -(du)_x - (dv)_y \tag{3}$$

$$u_t = -g\eta_x + fv - F^{(u)} + G^{(u)} \tag{4}$$

$$v_t = -g\eta_y - fu - F^{(v)} + G^{(v)} \tag{5}$$

where

$\eta(x,y,t)$ = elevation of water surface above mean level
$u(x,y,t)$ = depth-averaged velocity in x-direction
$v(x,y,t)$ = depth-averaged velocity in y-direction
$d(x,y)$ = mean water level
x,y = Cartesian coordinates in horizontal plane
f = Coriolis coefficient (assumed constant)
t = time

$F^{(u)}$ and $F^{(v)}$ represent friction terms. A quadratic bottom friction of the following form is used:

$$F^{(u)} = ku(u^2 + v^2)^{1/2}/d \; ; \; F^{(v)} = kv(u^2 + v^2)^{1/2}/d \tag{6}$$

where k is a dimensionless bottom friction coefficient. The terms $G^{(u)}$ and $G^{(v)}$ in equations (3) to (5) represent forcing terms, such as surface wind stress, equilibrium tide gradient, etc., which may vary with x,y,t. For storm surge computations, these terms will represent the meteorological forcing terms and for tidal computations, they represent the tidal potential. For the present problem of tsunami generation and propagation, these terms are ignored and the forcing comes in the form of an increasing water level directly above the bottom (of the ocean) displacement.

A simple Richardson grid (Figure 4) was chosen as the basis for the finite-difference scheme on the grounds that it minimizes storage and permits particularly simple

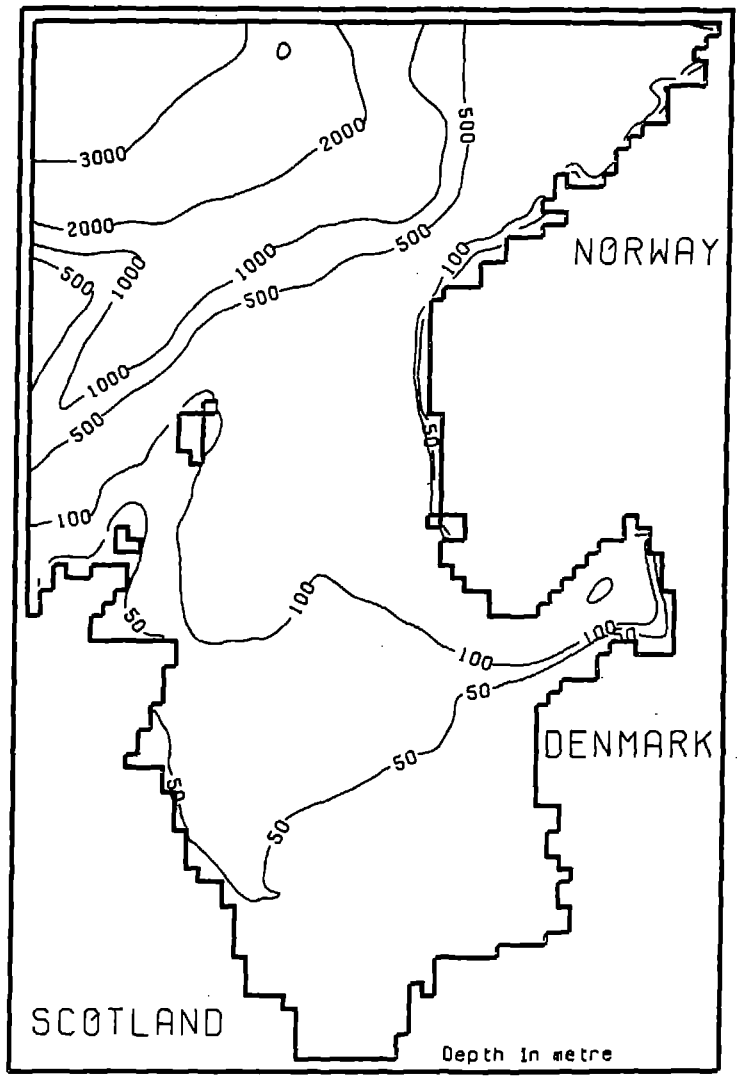

Figure 2 Water depths (m) in the computational domain of the numerical model.

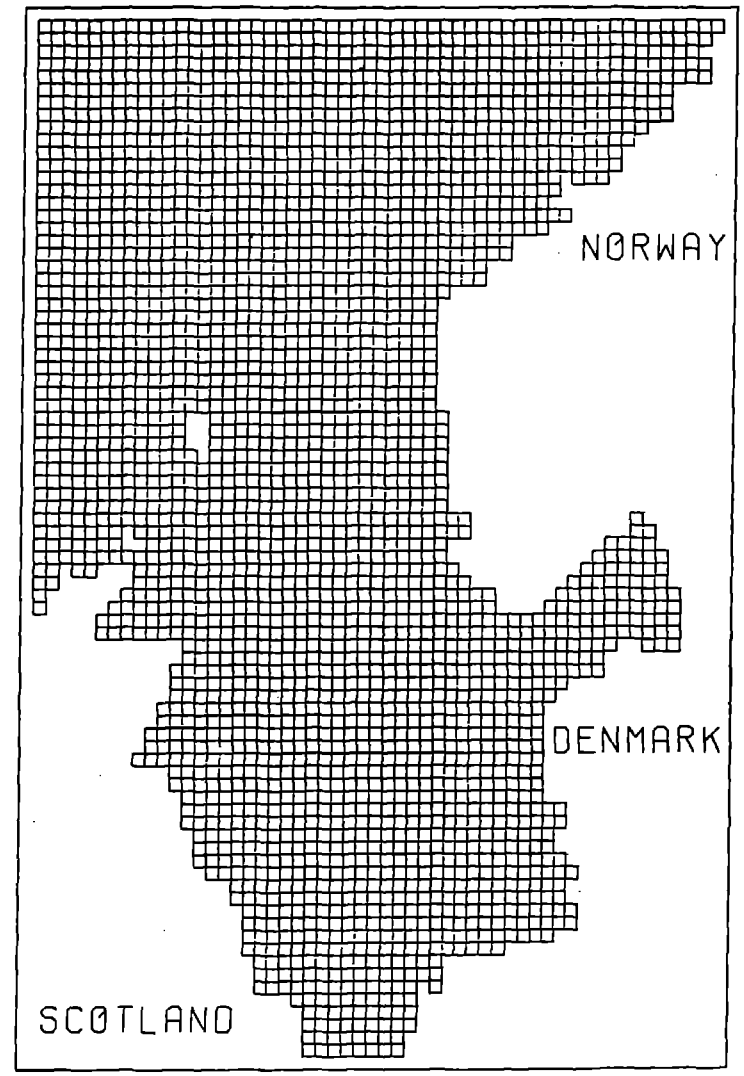

Figure 3 Computational grid of size 18.55 km.

representation of coastlines. At interior points of the grid, equations (3) to (5) are represented by the following finite-difference forms:

$$\frac{\eta'_{ij} - \eta_{ij}}{\Delta t} = - \frac{(d_{ij} + d_{i+1,j})u_{i+1,j} - (d_{i-1,j} + d_{ij})u_{ij}}{2\cdot\Delta x} - \frac{(d_{ij} + d_{i,j+1})v_{i,j+1} - (d_{i,j-1} + d_{ij})v_{ij}}{2\cdot\Delta y} \tag{7}$$

$$\frac{u'_{ij} - u_{ij}}{\Delta t} = -g \frac{\eta'_{ij} - \eta'_{i-1,j}}{\Delta x} + f\tilde{v}_{ij} - F^{(u)}_{ij} + G^{(u)}_{ij} \tag{8}$$

$$\frac{v'_{ij} - v_{ij}}{\Delta t} = - g \frac{\eta'_{ij} - \eta'_{i,j-1}}{\Delta y} - f\tilde{u}'_{ij} - F^{(v)}_{ij} + G^{(v)}_{ij} \tag{9}$$

where

Δt = time step
$\Delta x, \Delta y$ = grid interval sizes in x,y directions respectively
d_{ij} = mean water depth at elevation points η_{ij}

$$\tilde{u}_{ij} = \frac{1}{4} u_{i,j-1} + u_{i+1,j-1} + u_{ij} + u_{i+1,j} \tag{10}$$

$$\tilde{v}_{ij} = \frac{1}{4} v_{i-1,j} + v_{ij} + v_{i-1,j+1} + v_{i,j+1} \tag{11}$$

Primes indicate variables updated during the current time step; unprimed variables are those evaluated at the previous step. The use of old (unprimed) values of v in the Coriolis term in (8) and new (primed) values of u in the corresponding term in (9) is

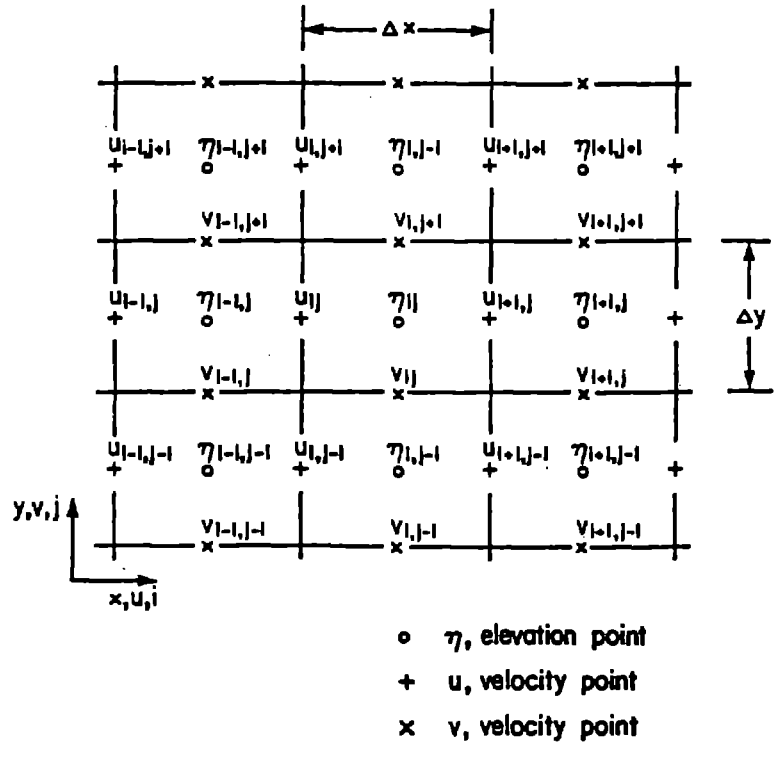

Figure 4 Computational scheme on the Richardson grid.

necessary for stability. Fortunately, it also eliminates the need to store any but the most recently updated values of each variable, provided that the equations are applied in the order given, that is, at each time step, all the η_{ij} are updated, then all the u_{ij}, and finally all the v_{ij}. The same stability and storage conclusions apply if variables are evaluated in the order η, v, u, using old values of u in the v-equation and new values of v in the u-equation. To reduce possible bias, the stepping subroutines evaluate the variables in the order η', v', u', on even-numbered steps.

Strictly speaking, equations (7) to (9) imply that u_{ij} and v_{ij} are evaluated $\Delta t/2$ later than η_{ij}, but normally they are regarded as pertaining to the same time level. The distinction is important only when calculating quantities which depend on phase differences

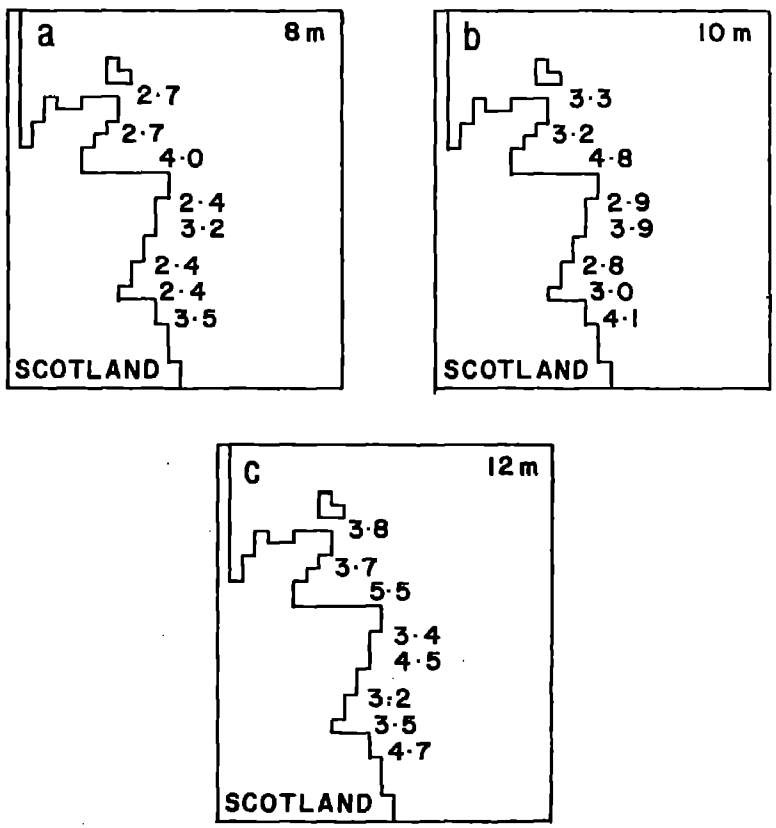

Figure 6 Maximum amplitude of the tsunami (m) for an initial maximum tsunami amplitude (at the source) of (a) 8m, (b) 10m and (c) 12m.

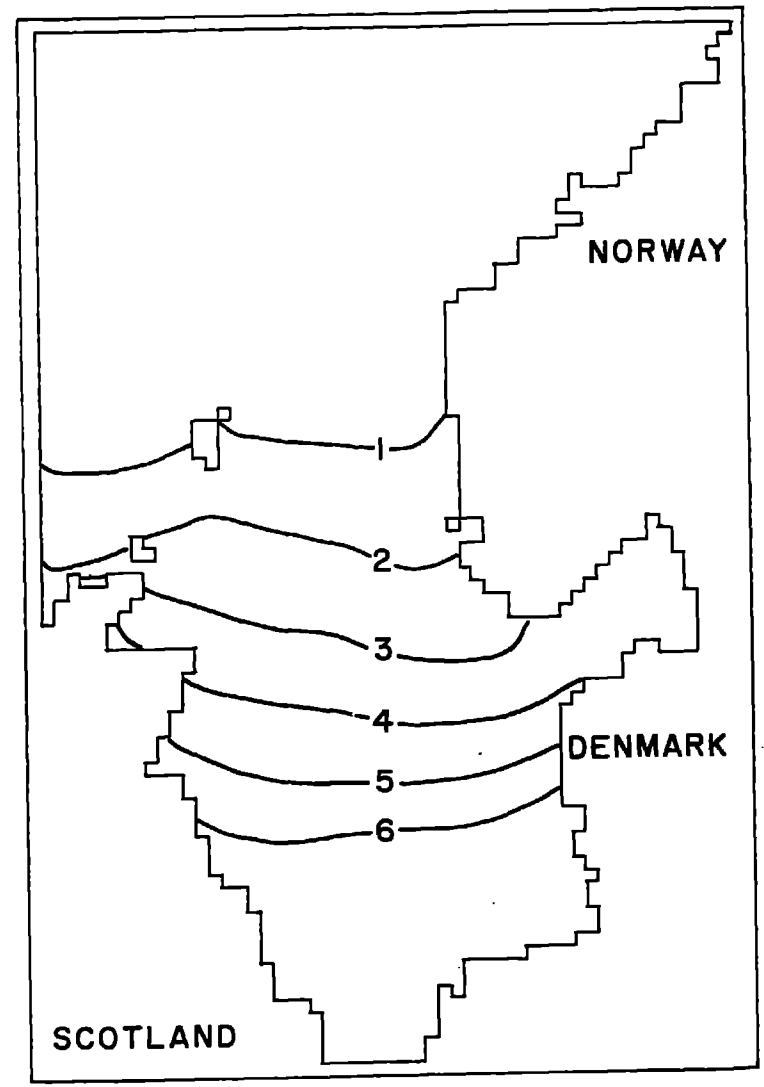

Figure 5 Position of the leading wave of the tsunami at hourly intervals.

between elevation and velocity, for example, energy flux, and then only when there are relatively few time steps per wave period.

A choice of a time step of 30 seconds satisfies the following stability criterion.

$$\Delta t \leq \frac{\Delta x \cdot \Delta y}{[g d_{max} (\Delta x^2 + \Delta y^2)]^{1/2}} \tag{12}$$

where d_{max} is the maximum depth in the computational region.

Where there are good grounds for assuming that no waves enter the model area from an adjacent water body, it is appropriate to use a radiation condition on the sea boundry between the two. This permits waves reaching the sea boundary from the interior of the model to pass out of the model domain (Henry, 1982).

When choosing the model grid initially, radiating sea boundaries parallel to the x-axis of the model should be placed to run through v-points on the grid. Similarly, those parallel to the y-axis should run ×through u-points. It is assumed that the radiation problem can be treated one-dimensionally at each velocity point on the sea boundry and thus that the surface elevation and normal velocity at the boundary are related by

$$\text{outward normal velocity} = (g/d)^{1/2} \times \text{elevation}$$

Since there are no elevation points actually on the boundary, the nearest interior elevation value is taken instead, so that the formulas used in the stepping subroutines for u-points on radiating boundaries facing in the positive or negative x-direction are respectively:

$$u_{ij} = (g/d_{i-1,j})^{1/2} \cdot \eta_{i-1,j}$$

or

$$u_{ij} = -(g/d_{ij})^{1/2} \cdot \eta_{ij}$$

Similarly, at radiating sea boundaries facing in the positive or negative y-directions, the formulas used are respectively:

or

$$v_{ij} = -(g/d_{ij})^{1/2} \cdot \eta_{ij}$$

$$v_{ij} = (g/d_{i,j-1})^{1/2} \cdot \eta_{i,j-1}$$

When this type of radiation boundary condition is used, the permissible time step may be reduced by 50%. Hence, in the stability criterion (12) the denominator should be multiplied by a factor of 2.

4. DISCUSSION OF RESULTS

It can be seen from Figure 5 that the tsunami takes about 2 hours to reach the northern tip of the east coast of Scotland and by about 6 hours the tsunami covers the area of interest of this study. Figure 6 shows the maximum amplitude of the tsunami on the east coast of Scotland at eight selected locations for an initial tsunami amplitude in the source region of (a) 8, (b) 10 and (c) 12 meters. These maximum tsunami amplitudes appear reasonable and certainly are in the range estimated by Dawson et al. (1988) and Long et al. (1989).

Our model has several shortcomings. Unlike Harbitz (1992) we did not simulate the slide and the initial aspects of tsunami generation. Nevertheless, the model yields results that appear to be in reasonable agreement with observations.

ACKNOWLEDGMENTS

We thank Drs. David Smith and Alistair Dawson for introducing us to this interesting problem. Mr. D.K. Lee did the computer programming, Mrs. C. Wallace drafted the diagrams and Mrs. N. Delacretaz typed the manuscript.

REFERENCES

Dawson, A.G., D. Long and D.E. Smith (1988) The Storegga slides: Evidence from eastern Scotland for a possible tsunami, Marine Geology, **82**, 271-276.

Harbitz, C.B. (1992) Model simulations of tsunamis generated by the Storegga slides, Marine Geology, **105**, 1-21.

Henry, R.F. (1982) Automated programming of explicit shallow water models: Part I. Linearized models with linear or quadratic friction, Can, Tech. Rept. Hydrogr. Ocean Sci. No. 3, Institute of Ocean Sciences, Dept. of Fisheries and Oceans, Sidney, B.C., Canada, 70p.

Jansen, E., S. Befring, T. Bugge, T. Eidvin, H. Holtedahl and H.P. Sejrup (1987) Large submarine slides on the Norwegian continental margin: Sediments transport and timing. Marine Geology, **78**, 77-107.

Long, D., D.E. Smith and A.G. Dawson (1989) A Holocene tsunami deposit in eastern Scotland, J. of Quaternary Science, **4**, 61-66.

Murty, T.S. (1977) Seismic sea waves – Tsunamis, Bull. 198, Fisheries Res. Board of Canada, Ottawa, 337p

Murty. T.S. (1979) Submarine slide-generated water waves in Kitimat Inlet, British Columbia, J. Geophys. Res., **84**(C12), 7777-7779.

Murty, T.S. (1984) Storm surges – Meteorological ocean tides, Bull. No. 212, Canadian Bull.of Fisheries and Aquatic Sciences, Ottawa, 906p.

Raney, D.C. and H.L. Butler (1975) A numerical model for predicting the effects of landslide generated water waves, Res. Rept. H-75-1, Feb. 1975, Waterways Expt. Station, Vicksburg, MS, 25p.

Slingerland, R. and B. Voight (1982) Evaluating hazard of land-slide induced water waves, J. Waterway Port Coastal and Ocean Engineering, Proc. Amer. Soc. Civil Engrs., **108**, WW4, 504-512.

Striem, H.L. and T. Miloh (1975) Tsunamis induced by submarine slumpings off the coast of Israel, Rept. of The Israel Atomic Energy Commission, 23p.

Wang, S.H., B. Le Mehaute and C.C. Lu (1987) Effect of dispersion on impulsive waves, Marine Geophys. Res., **9**, 95-111.

Wigen, S.O., T.S. Murty and D.G. Philip (1983) Tsunami of May 11, 1981, on the coast of South Africa, Proc. 1983 Tsunami Symp., Hamburg, Ed: E.N. Bernard, 187-202.

TSUNAMI '93
Disaster Prevention Research Institute
Kyoto University, Uji, Kyoto 611, Japan

INTERNATIONAL TSUNAMI SYMPOSIUM

The International Tsunami Symposium, Tsunami '93 of the Tsunami Commission of the International Union of Geodesy and Geophysics will be held in **Wakayama, Japan on August 23-27, 1993.** The workshop on the Technical Aspects of Tsunami Analysis, Prediction and Communications will be also held in the period. The symposium is organized by the Local Organizing Committee of the Japan Society of Civil Engineers.

The symposium will be held at Wakayama Tokyu Inn in Wakayama City. Wakayama is one of the most historical areas in the prevention of tsunami disasters in Japan(see the reverse side). The city is located 60km south of Osaka. It takes only one hour from Osaka and four hours from Tokyo by train.

Social and recreational programs and a post symposium technical tour are being arranged for accompanied persons as well as for the participants in the scientific and technical sessions.

The symposium proceedings will be published and distributed to the participants at the symposium. Only camera-ready full manuscripts will be accepted. The author(s) is obliged to present orally at the symposium. Those interested in attending are invited to complete the form below and return it to the above address as soon as possible so they may receive more information.

APPLICATION FOR MEMBERSHIP

THE TSUNAMI SOCIETY
P.O. Box 8523
Honolulu, Hawaii 96815, USA

I desire admission into the Tsunami Society as: (Check appropriate box.)

☐ Student ☐ Member ☐ Institutional Member

Name _____ Signature _____

Address _____ Phone No. _____

_____

Zip Code _____ Country _____

Employed by _____

Address _____

Title of your position _____

FEE: Student $5.00 Member $25.00 Institution $100.00

Fee includes a subscription to the society journal: SCIENCE OF TSUNAMI HAZARDS.

Send dues for one year with application. Membership shall date from 1 January of the year in which the applicant joins. Membership of an applicant applying on or after October 1 will begin with 1 January of the succeeding calendar year and his first dues payment will be applied to that year.